Metastability in a Stochastic Neural Network Modeled as a Velocity Jump Markov Process[*]

Paul C. Bressloff[†] and Jay M. Newby[‡]

Abstract. One of the major challenges in neuroscience is to determine how noise that is present at the molecular and cellular levels affects dynamics and information processing at the macroscopic level of synaptically coupled neuronal populations. Often noise is incorporated into deterministic network models using extrinsic noise sources. An alternative approach is to assume that noise arises intrinsically as a collective population effect, which has led to a master equation formulation of stochastic neural networks. In this paper we extend the master equation formulation by introducing a stochastic model of neural population dynamics in the form of a velocity jump Markov process. The latter has the advantage of keeping track of synaptic processing as well as spiking activity, and reduces to the neural master equation in a particular limit. The population synaptic variables evolve according to piecewise deterministic dynamics, which depends on population spiking activity. The latter is characterized by a set of discrete stochastic variables evolving according to a jump Markov process, with transition rates that depend on the synaptic variables. We consider the particular problem of rare transitions between metastable states of a network operating in a bistable regime in the deterministic limit. Assuming that the synaptic dynamics is much slower than the transitions between discrete spiking states, we use a WKB approximation and singular perturbation theory to determine the mean first passage time to cross the separatrix between the two metastable states. Such an analysis can also be applied to other velocity jump Markov processes, including stochastic voltage-gated ion channels and stochastic gene networks.

1. Introduction.

Noise has recently emerged as a key component of many biological systems, including the brain. Stochasticity arises at multiple levels of brain function, ranging from molecular processes such as gene expression and the opening of ion channel proteins to complex networks of noisy spiking neurons that generate behavior [28]. For example, the spike trains of individual cortical neurons *in vivo* tend to be very noisy, having interspike interval (ISI) distributions that are close to Poisson [75]. At the network level, noise appears to be present during perceptual decision making [82] and bistable perception, the latter being exemplified by perceptual switching during binocular rivalry [53, 74, 84]. Noise also contributes to the generation of spontaneous activity during resting states [23, 22]. At the level of large-scale

neural systems, as measured with functional MRI (fMRI) imaging, this ongoing spontaneous activity reflects the organization of a series of highly coherent functional networks that may play an important role in cognition. One of the major challenges in neuroscience is to develop our understanding of how noise that is present at the molecular and cellular levels affects dynamics and information processing at the macroscopic level of synaptically coupled neuronal populations. Mathematical and computational modeling are playing an increasing role in developing such an understanding [45].

Following studies of biochemical and gene networks [77, 28], it is useful to make the distinction between intrinsic and extrinsic noise sources. Extrinsic noise refers to external sources of randomness associated with environmental factors, and is often modeled as a continuous Markov process based on Langevin equations. On the other hand, intrinsic noise typically refers to random fluctuations arising from the discrete and probabilistic nature of chemical reactions at the molecular level, which are particularly significant when the number of reacting molecules N is small. Under such circumstances, the traditional approach to modeling chemical reactions based on the law of mass action is inappropriate. Instead, a master equation formulation is necessary in order to describe the underlying jump Markov process. In the case of single cortical neurons, the main source of extrinsic noise arises from synaptic inputs. That is, cortical neurons are being constantly bombarded by thousands of synaptic currents, many of which are not correlated with a meaningful input and can thus be treated as background synaptic noise. The main source of intrinsic fluctuations at the single-cell level is channel noise, which arises from the variability in the opening and closing of a finite number of ion channels. The resulting conductance-based model of a neuron can be formulated as a stochastic hybrid system, in which a piecewise smooth deterministic dynamics describing the time evolution of the membrane potential is coupled to a jump Markov process describing channel dynamics [66, 15, 61].

It is not straightforward to determine how noise at the single-cell level translates into noise at the population or network level. A number of methods involve carrying out some form of dimension reduction of a network of synaptically coupled spiking neurons. These include population density methods [62, 64, 47], mean-field theories [1, 36, 14, 13, 2], and Boltzmann-like kinetic theories [20, 69, 19]. However, such methods tend to consider either fully connected or sparsely connected networks and simplified models of spiking neurons such as the integrate-and-fire (IF) model. Nevertheless, one interesting result that emerges from the mean-field analysis of IF networks is that, under certain conditions, even though individual neurons exhibit Poisson-like statistics, the neurons fire asynchronously so that the total population activity evolves according to a mean-field rate equation with a characteristic activation or gain function [1, 36, 14, 13, 71]. Formally speaking, the asynchronous state exists only in the thermodynamic limit $N \to \infty$, where N determines the size of the population. This then suggests a possible source of intrinsic noise at the network level arises from fluctuations about the asynchronous state due to finite size effects [52, 50, 76, 6]; this is distinct from intrinsic noise at the single-cell level due to channel fluctuations, and it is assumed that the latter is negligible at the population level. The presence of finite-size effects has motivated developing a closer analogy between intrinsic noise in biochemical and neural networks [7, 8], based on a rescaled version of the neural master equation introduced by Buice et al. [17, 18]; see also [63].

In the Buice et al. master equation [17, 18], neurons are partitioned into a set of M lo-

cal homogeneous populations. The state of the αth population at time t is specified by the number $N_\alpha(t)$ of active (spiking) neurons in an infinite background sea of inactive neurons. (This is reasonable if the networks are in low activity states.) Transitions between the states are given by a one-step jump Markov process, with the transition rates chosen so that standard Wilson–Cowan or activity-based equations are obtained in the mean-field limit, where statistical correlations can be ignored. One of the features of the Buice et al. master equation is that there does not exist a natural small parameter, so that it is not possible to carry out a diffusion-like approximation using, for example, a system-size expansion. Indeed, the network tends to operate in a regime close to Poisson-like statistics. Nevertheless, it is possible to solve the moment hierarchy problem using either path-integral methods or factorial moments [17, 18]. In contrast, the Bressloff master equation [7, 8] assumes that there is a finite number N of neurons in each local population and characterizes the state of each population in terms of the fraction of neurons $N_\alpha(t)/N$ that have spiked in an interval of width Δt. The transition rates are rescaled so that in the thermodynamic limit $N \to \infty$, one recovers the Wilson–Cowan mean-field equations. For large but finite N, the network operates in a Gaussian-like regime that can be described in terms of an effective neural Langevin equation [7, 8]. One of the advantages of this version of the master equation from a mathematical perspective is that a variety of well-established methods from the analysis of chemical master equations can be generalized to the neural case. For example, a rigorous analysis of the Langevin approximation can be carried out [16] by extending the work of Kurtz [43] on chemical master equations. Moreover, Wentzel–Kramers–Brillouin (WKB) methods can be used to analyze rare transitions between metastable states, for which the Langevin approximation breaks down [8]. For a discussion of the differences between the two master equations from the perspective of corrections to mean-field theory, see [79].

In this paper we go beyond the neural master equations by formulating the network population dynamics in terms of a stochastic hybrid system also known as a "velocity" jump Markov process. This generalization is motivated by a major limitation of the neural master equations. That is, they neglect synaptic dynamics completely, keeping track of changes only in spiking activity. This implies, for example, that the relaxation time τ for synaptic dynamics is much smaller than the fundamental time step Δt for jumps in the number of active neurons. Our model associates with each population two stochastic variables $U_\alpha(t)$ and $N_\alpha(t)$. The synaptic variables $U_\alpha(t)$ evolve according to piecewise–deterministic dynamics describing, at the population level, synapses driven by spiking activity. These equations are only valid between jumps in spiking activity, which are described by a jump Markov process whose transition rates depend on the synaptic variables. We then show how asymptotic methods recently developed to study metastability in stochastic ion channels, motor-driven intracellular cargo transport, and gene networks [58, 61, 55, 56] can be extended to analyze metastability in stochastic neural networks. All of these systems are modeled in terms of a stochastic hybrid system. For example, in the case of ion channels, N_α would represent the number of open channels of type α, whereas U_α would be replaced by the membrane voltage V. On the other hand, for intracellular transport, N_α would be the number of motors of type α actively transporting a cargo and U_α would be replaced by position X along the track.

The structure of the paper is as follows. In section 2, we construct our stochastic network model. We then analyze bistability in a one-population model (section 3), and a two-

population model consisting of a pair of excitatory and inhibitory networks (section 4). In both cases, we carry out an eigenfunction expansion of the probability density and equate the principal eigenvalue with the inverse mean first passage time from one metastable state to the other. The principal eigenvalue is expressed in terms of the inner product of a quasistationary density and an adjoint eigenfunction. The former is evaluated using a WKB approximation, whereas the latter is determined using singular perturbation theory, in order to match an absorbing boundary condition on the separatrix between the basins of attraction of the two metastable states. In the two-population case, calculating the effective potential of the quasistationary density requires identifying an appropriate Hamiltonian system, which turns out to be nontrivial, since the system does not satisfy detailed balance.

A number of general comments are in order before proceeding further.

(i) There does not currently exist a rigorous derivation of population rate–based models starting from detailed biophysical models of individual neurons. Therefore, the construction of the stochastic rate–based model in section 2 is heuristic in nature, in order to motivate the neural rate equations used in this paper.

(ii) We use formal asymptotic methods rather than rigorous stochastic analysis to determine the transition rates between metastable states in sections 3 and 4, and we validate our approach by comparing with Monte Carlo simulations. Such methods have been applied extensively to Fokker–Planck (FP) equations and master equations as reviewed in [72] and provide useful insights into the underlying dynamical processes. In this paper we extend these methods to a stochastic hybrid system. One could develop a more rigorous approach using large deviation theory [31, 30, 80], for example. However, large deviation theory does not generate explicit expressions for the prefactor, which we find can contribute significantly to the transition rates.

(iii) We focus on networks operating in the bistable regime, where the simpler quasi-steady-state diffusion approximation breaks down, in the sense that it yields exponentially large errors in the transition rates. There are a growing number of examples of bistability in systems neuroscience, including transitions between cortical up and down states during slow wave sleep [21, 68], working memory [38], and ambiguous perception as exemplified by binocular rivalry [3, 53, 44, 12]. On the other hand, in the case of oscillator networks, a diffusion approximation combined with Floquet theory might be sufficient to capture the effects of noise, including the noise-induced amplification of coherent oscillations or quasicycles [51, 4, 8]. An interesting issue is whether or not the WKB method and matched asymptotics can be applied to a network operating in an excitable regime, where there is a stable low activity resting state such that noninfinitesimal perturbations can induce a large excursion in phase space before returning to the resting state. One of the difficulties with excitable systems is that there does not exist a well-defined separatrix. Nevertheless, it is possible to extend the asymptotic methods developed here to the excitable case, as we will show elsewhere within the context of spontaneous action potential generation in a model of an excitable conductance-based neuron with stochastic ion channels [60].

2. Stochastic network model and the Chapman–Kolmogorov equation.
Suppose that a network of synaptically coupled spiking neurons is partitioned into a set of M homogeneous populations with N neurons in each population, $\alpha = 1, \ldots, M$. (A straightforward general-

ization would be take to take each population to consist of $\mathcal{O}(N)$ neurons.) Let χ denote the population function that maps the single neuron index $i = 1, \ldots, NM$ to the population index α to which neuron i belongs: $\chi(i) = \alpha$. Furthermore, suppose the synaptic interactions between populations are the same for all neuron pairs. (Relaxing this assumption can lead to additional sources of stochasticity as explored in [29, 78].) Denote the sequence of firing times of the jth neuron by $\{T_j^m, m \in \mathbf{Z}\}$. The net synaptic current into postsynaptic neuron i due to stimulation by the spike train from presynaptic neuron j, with $\chi(i) = \alpha, \chi(j) = \beta$, is taken to have the general form $N^{-1} \sum_m \Phi_{\alpha\beta}(t - T_j^m)$, where $N^{-1}\Phi_{\alpha\beta}(t)$ represents the temporal filtering effects of synaptic and dendritic processing of inputs from any neuron of population β to any neuron of population α. For concreteness, we will take exponential synapses so that

$$(2.1) \qquad \Phi_{\alpha\beta}(t) = w_{\alpha\beta}\Phi(t), \quad \Phi(t) = \tau^{-1}\mathrm{e}^{-t/\tau}H(t).$$

(A more general discussion of different choices for $\Phi_{\alpha\beta}(t)$ can be found in the reviews of [26, 9].) Assuming that all synaptic inputs sum linearly, the total synaptic input to the soma of the ith neuron, which we denote by $u_i(t)$, is

$$(2.2) \qquad u_i(t) = \sum_{\beta} \frac{1}{N} \sum_{j;\chi(j)=\beta} \Phi_{\alpha\beta}(t - T_j^m) = \int_{-\infty}^{t} \sum_{\beta} \Phi_{\alpha\beta}(t - t') \frac{1}{N} \sum_{j;\chi(j)=\beta} a_j(t')dt'$$

for all $\chi(i) = \alpha$, where

$$(2.3) \qquad a_j(t) = \sum_{m \in \mathbf{Z}} \delta(t - T_j^m).$$

That is, $a_j(t)$ represents the output spike train of the jth neuron in terms of a sum of Dirac delta functions. (Note that in (2.2) we are neglecting any i-dependent transients arising from initial conditions, since these decay exponentially for any biophysically based model of the kernels $\Phi_{\alpha\beta}$.) In order to obtain a closed set of equations, we have to determine threshold conditions for the firing times T_i^m. These take the form

$$(2.4) \qquad T_i^m = \inf\left\{t, t > T_i^{m-1}\,\middle|\, V_i(t) = \kappa_{\mathrm{th}}, \frac{dV_i}{dt} > 0\right\},$$

where κ_{th} is the firing threshold and $V_i(t)$ is the somatic membrane potential. The latter is taken to evolve according to a conductance-based model

$$(2.5) \qquad C\frac{dV_i}{dt} = -I_{\mathrm{con,i}}(V_i, \ldots) + u_i,$$

which is supplemented by additional equations for a set of ionic gating variables [27]. (The details of the conductance-based model will not be important for the subsequent analysis.) Let $a_\alpha(t)$ denote the output activity of the αth population,

$$(2.6) \qquad a_\alpha(t) = \frac{1}{N} \sum_{j;\chi(j)=\alpha} a_j(t),$$

and rewrite (2.2) as

$$u_i(t) = \int_{-\infty}^t \sum_\beta \Phi_{\alpha\beta}(t - t')a_\beta(t')dt', \quad \chi(i) = \alpha.$$

Since the right-hand side is independent of i, it follows that $u_i(t) = u_\alpha(t)$ for all $\chi(i) = \alpha$ with

$$(2.7) \qquad u_\alpha(t) = \sum_{\beta=1}^M \int_{-\infty}^t \Phi_{\alpha\beta}(t - t')a_\beta(t')dt'.$$

In the case of exponential synapses (2.1), equation (2.7) can be converted to the differential equation

$$(2.8) \qquad \tau\frac{du_\alpha}{dt} = -u_\alpha(t) + \sum_{\beta=1}^M w_{\alpha\beta}a_\beta(t).$$

In general, (2.2)–(2.5) are very difficult to analyze. However, considerable simplification can be obtained if the total synaptic current $u_i(t)$ is slowly varying compared to the membrane potential dynamics given by (2.5). This would occur, for example, if each of the homogeneous subnetworks fired asynchronously [35]. One is then essentially reinterpreting the population activity variables $u_\alpha(t)$ and $a_\alpha(t)$ as mean fields of local populations. (Alternatively, a slowly varying synaptic current would occur if the synapses are themselves sufficiently slow [25, 10].) These simplifying assumptions motivate replacing the output population activity by an instantaneous firing rate $a_\alpha(t) = F(u_\alpha(t))$ with F identified as the so-called population gain function. Equation (2.7) then forms the closed system of integral equations

$$(2.9) \qquad u_\alpha(t) = \int_{-\infty}^t \sum_\beta \Phi_{\alpha\beta}(t - t')F(u_\beta(t'))dt'.$$

The basic idea is that if neurons in a local population are firing asynchronously, then the output activity a_α is approximately constant, which means that the synaptic currents are also slowly varying functions of time. A nonlinear relationship between a_α and constant input current u_α can then be derived using population averaging in order to determine the gain function F. One then assumes that the same relationship $a_\alpha = F(u_\alpha)$ also holds for time-dependent synaptic currents, provided that the latter vary slowly with time. In certain cases F can be calculated explicitly [1, 36, 14, 13]. Typically, a simple model of a spiking neuron is used, such as the IF model [35], and the network topology is assumed to be either fully connected or sparsely connected. It can then be shown that under certain conditions, even though individual neurons exhibit Poisson-like statistics, the neurons fire asynchronously so that the total population activity evolves according to a mean-field rate equation with a characteristic gain function F. In practice, however, it is sufficient to approximate the firing rate function by a sigmoid:

$$(2.10) \qquad F(u) = \frac{F_0}{1 + e^{-\gamma(u-\kappa)}},$$

where γ, κ correspond to the gain and threshold respectively.

One of the goals of this paper is to develop a generalization of the neural master equation [17, 18, 7] that incorporates synaptic dynamics. We proceed by taking the output activity of a local homogeneous population to be a discrete stochastic variable $A_\alpha(t)$ rather than the instantaneous firing rate $a_\alpha = F(u_\alpha)$:

$$(2.11) \qquad A_\alpha(t) = \frac{N_\alpha(t)}{N\Delta t},$$

where $N_\alpha(t)$ is the number of neurons in the αth population that fired in the time interval $[t - \Delta t, t]$, and Δt is the width of a sliding window that counts spikes. The discrete stochastic variables $N_\alpha(t)$ are taken to evolve according to a one-step jump Markov process:

$$(2.12) \qquad N_\alpha(t) \to N_\alpha(t) \pm 1 : \quad \text{transition rate } \Omega_\pm(U_\alpha(t), N_\alpha(t)),$$

with the synaptic current $U_\alpha(t)$ given by (for exponential synapses)

$$(2.13) \qquad \tau dU_\alpha(t) = \left[-U_\alpha(t) + \sum_{\beta=1}^M w_{\alpha\beta} A_\beta(t) \right] dt.$$

The transition rates are taken to be (cf. [7])

$$(2.14) \qquad \Omega_+(u_\alpha, n_\alpha) \to \Omega_+(u_\alpha) = \frac{N\Delta t}{\tau_a} F(u_\alpha), \quad \Omega_-(u_\alpha, n_\alpha) \to \Omega_-(n_\alpha) = \frac{n_\alpha}{\tau_a}.$$

The resulting stochastic process defined by (2.13), (2.11), (2.12), and (2.14) is an example of a stochastic hybrid system based on a piecewise deterministic process. That is, the transition rate Ω_+ depend on U_α, with the latter itself coupled to the associated jump Markov according to (2.13), which is only defined between jumps, during which $U_\alpha(t)$ evolves deterministically. (Stochastic hybrid systems also arise in applications to genetic networks [85, 56] and to excitable neuronal membranes [66, 15, 41].) It is important to note that the time constant τ_a cannot be identified directly with membrane or synaptic time constants. Instead, it determines the relaxation rate of a local population to the instantaneous firing rate.

2.1. Neural master equation. Previous studies of the neural jump Markov process have effectively taken the limit $\tau \to 0$ in (2.13) so that the continuous variables $U_\alpha(t)$ are eliminated by setting $U_\alpha(t) = \sum_\beta w_{\alpha\beta} A_\alpha(t)$. This then leads to a pure birth–death process for the discrete variables $N_\alpha(t)$. That is, let $P(\mathbf{n}, t) = \text{Prob}[\mathbf{N}(t) = \mathbf{n}]$ denote the probability that the network of interacting populations has configuration $\mathbf{n} = (n_1, n_2, \ldots, n_M)$ at time $t, t > 0$, given some initial distribution $P(\mathbf{n}, 0)$ with $0 \le n_\alpha \le N$. The probability distribution then evolves according to the birth–death master equation [17, 18, 7]

$$(2.15) \qquad \frac{dP(\mathbf{n}, t)}{dt} = \sum_\alpha \left[(\mathbb{T}_\alpha - 1) \left(\Omega_\alpha^-(\mathbf{n}) P(\mathbf{n}, t) \right) + (\mathbb{T}_\alpha^{-1} - 1) \left(\Omega_\alpha^+(\mathbf{n}) P(\mathbf{n}, t) \right) \right],$$

where

$$(2.16) \qquad \Omega_\alpha^+(\mathbf{n}) = \frac{N\Delta t}{\tau_a} F\left(\sum_\beta w_{\alpha\beta} n_\alpha / N\Delta t \right), \quad \Omega_\alpha^-(\mathbf{n}) = \frac{n_\alpha}{\tau_a},$$

and $\mathbb{T}_\alpha$ is a translation operator: $\mathbb{T}_\alpha^{\pm 1} F(\mathbf{n}) = F(\mathbf{n}_{\alpha\pm})$ for any function F with $\mathbf{n}_{\alpha\pm}$ denoting the configuration with n_α replaced by $n_\alpha \pm 1$. Equation (2.15) is supplemented by the boundary conditions $P(\mathbf{n}, t) \equiv 0$ if $n_\alpha = N + 1$ or $n_\alpha = -1$ for some α. The birth–death master equation (2.15) can be analyzed by adapting various methods from the analysis of chemical master equations including system-size expansions, WKB approximations, and path integral representations [18, 7, 8, 16]. First, suppose that we fix $\Delta t = 1$ so that we obtain the Bressloff version of the master equation. Taking the thermodynamic limit $N \to \infty$ then yields the deterministic activity-based mean-field equation

$$(2.17) \qquad \tau_\alpha \frac{dA_\alpha}{dt} = -A_\alpha(t) + F\left(\sum_\beta w_{\alpha\beta} A_\alpha(t)\right).$$

(For a detailed discussion of the differences between activity-based and voltage-based neural rate equations, see [27, 9].) For large but finite N, the master equation (2.15) can be approximated by an FP equation using a Kramers–Moyal or system-size expansion, so that the population activity A_α evolves according to a Langevin equation [7]. A rigorous probabilistic treatment of the thermodynamic limit of the neural master equation has also been developed [16], extending previous work on chemical master equations [42]. Although the diffusion approximation can capture the stochastic dynamics of the neural population at finite times, it can break down in the limit $t \to \infty$. For example, suppose that the deterministic system (2.17) has multiple stable fixed points. The diffusion approximation can then account for the effects of fluctuations well within the basin of attraction of a locally stable fixed point. However, there is now a small probability that there is a noise-induced transition to the basin of attraction of another fixed point. Since the probability of such a transition is usually on the order of e^{-cN}, $c = \mathcal{O}(1)$, except close to the boundary of the basin of attraction, such a contribution cannot be analyzed accurately using standard FP methods [81]. These exponentially small transitions play a crucial role in allowing the network to approach the unique stationary state (if it exists) in the asymptotic limit $t \to \infty$, and can be analyzed using a WKB approximation of the master equation together with matched asymptotics [8]. In other words, for a multistable neural system, the limits $t \to \infty$ and $N \to \infty$ do not commute, as previously noted for chemical systems [39].

Now suppose that we take the limit $N \to \infty, \Delta t \to 0$ such that $N\Delta t = 1$. We then recover the neural master equation of Buice et al. [17, 18]. In this case there is no small parameter that allows us to construct a Langevin approximation to the master equation. Nevertheless, it is possible to determine the moment hierarchy of the master equation using path-integral methods or factorial moments, based on the observation that the network operates in a Poisson-like regime. The role of the sliding window size Δt is crucial in understanding the difference between the two versions of the master equation. First, it should be emphasized that the stochastic models are keeping track of *changes* in population spiking activity. If the network is operating close to an asynchronous state for large N, then one-step changes in population activity could occur relatively slowly so there is no need to take the limit $\Delta t \to 0$. On the other hand, if population activity is characterized by a Poisson process, then it is necessary to take the limit $\Delta t \to 0$ in order to maintain a one-step process. However, given the existence of an arbitrarily small time-scale Δt, it is no longer clear that one is

justified in ignoring synaptic dynamics by taking the limit $\tau \to 0$ in (2.13). This observation motivates the approach taken in this paper, in which we incorporate synaptic dynamics into the neural master equation. In the following, we will assume that the network operates in the Poisson-like regime in the absence of synaptic dynamics.

2.2. Neural Chapman–Kolmogorov equation. Let us now return to the full stochastic hybrid system. Introduce the probability density

$$(2.18) \qquad \text{Prob}\{U_\alpha(t) \in (u_\alpha, u_\alpha + du, N_\alpha(t) = n_\alpha; \alpha = 1, \ldots, M\} = p(\mathbf{u}, \mathbf{n}, t | \mathbf{u}_0, \mathbf{n}_0, 0) d\mathbf{u},$$

with $\mathbf{u} = (u_1, \ldots, u_M)$ and $\mathbf{n} = (n_1, \ldots, n_M)$. It follows from (2.11), (2.12), (2.13), and (2.14) that the probability density evolves according to the differential Chapman–Kolmogorov (CK) equation (dropping the explicit dependence on initial conditions)

$$(2.19) \qquad \frac{\partial p}{\partial t} + \frac{1}{\tau} \sum_\alpha \frac{\partial [v_\alpha(\mathbf{u}, \mathbf{n}) p(\mathbf{u}, \mathbf{n}, \mathbf{t})]}{\partial u_\alpha}$$
$$= \frac{1}{\tau_a} \sum_\alpha \left[(\mathbb{T}_\alpha - 1) \left(\omega_-(n_\alpha) p(\mathbf{u}, \mathbf{n}, t) \right) + (\mathbb{T}_\alpha^{-1} - 1) \left(\omega_+(u_\alpha) p(\mathbf{u}, \mathbf{n}, \mathbf{t}) \right) \right],$$

with

$$(2.20) \qquad \omega_+(u_\alpha) = F(u_\alpha), \quad \omega_-(n_\alpha) = n_\alpha, \quad v_\alpha(\mathbf{u}, \mathbf{n}) = -u_\alpha + \sum_\beta w_{\alpha\beta} n_\beta.$$

We have taken the limit $N \to \infty$, $\Delta t \to 0$ with $N\Delta t = 1$. Note that (2.19) can be re-expressed in the more general form

$$(2.21) \qquad \frac{\partial p}{\partial t} = -\frac{1}{\tau} \sum_{\alpha=1}^M \frac{\partial}{\partial u_\alpha} (v_\alpha(\mathbf{u}, \mathbf{n}) p(\mathbf{u}, \mathbf{n}, t)) + \frac{1}{\tau_a} \sum_{\mathbf{m}} A(\mathbf{n}, \mathbf{m}; \mathbf{u}) p(\mathbf{u}, \mathbf{m}, t).$$

The drift "velocities" $v_\alpha(\mathbf{u}, \mathbf{n})$ for fixed $\mathbf{n}$ represent the piecewise-deterministic synaptic dynamics according to

$$(2.22) \qquad \tau \frac{du_\alpha}{dt} = v_\alpha(\mathbf{u}, \mathbf{n}), \quad \alpha = 1, \ldots, M,$$

and A represents the $\mathbf{u}$-dependent transition matrix for the jump Markov process. For fixed $\mathbf{u}$, the matrix $A(\mathbf{n}, \mathbf{m}; \mathbf{u})$ is irreducible (which means that there is a nonzero probability of transitioning, possibly in more than one step, from any state to any other state in the jump Markov process) and has a simple zero eigenvalue. In particular, $\sum_{\mathbf{n}} A(\mathbf{n}, \mathbf{m}; \mathbf{u}) = 0$ for all $\mathbf{m}$, that is, $\mathbf{n} = (1, 1, \ldots, 1)^T$ is the left null vector of A. The Perron–Frobenius theorem ensures that all other eigenvalues of A are negative, and the continuous-time Markov process for fixed $\mathbf{u}$,

$$\frac{dp(\mathbf{u}, \mathbf{n}, t)}{dt} = \frac{1}{\tau_a} \sum_{\mathbf{m} \in I} A(\mathbf{n}, \mathbf{m}; \mathbf{u}) p(\mathbf{u}, \mathbf{m}, t),$$

has a globally attracting steady-state $\rho(\mathbf{u}, \mathbf{n})$ such that $p(\mathbf{u}, \mathbf{n}, t) \to \rho(\mathbf{u}, \mathbf{n})$ as $t \to \infty$. The steady-state equation is

$$0 = \sum_{\mathbf{m}} A(\mathbf{n}, \mathbf{m}; \mathbf{u})\rho(\mathbf{u}, \mathbf{m})$$

$$= \sum_{\alpha=1}^{M} [(n_\alpha + 1)\rho(\mathbf{u}, \mathbf{n} + \mathbf{e}_\alpha) - n_\alpha\rho(\mathbf{u}, \mathbf{n}) + F(u_\alpha)(\rho(\mathbf{u}, \mathbf{n} - \mathbf{e}_\alpha) - \rho(\mathbf{u}, \mathbf{n}))],$$

where $[\mathbf{e}_\alpha]_\beta = \delta_{\alpha,\beta}$. The solution can be factorized as $\rho(\mathbf{u}, \mathbf{n}) = \prod_{\beta=1}^{M} \rho_1(u_\beta, n_\beta)$ with

$$0 = \sum_{\alpha=1}^{M} \left[\prod_{\beta \neq \alpha} \rho_1(u_\beta, n_\beta) \right] [J(u_\alpha, n_\alpha + 1) - J(u_\alpha, n_\alpha)],$$

where

$$J(u, n) = n\rho_1(u, n) - F(u)\rho_1(u, n - 1).$$

Since $\rho_1(u, -1) \equiv 0$, it follows that $J(u, n) = 0$ for all n. Hence,

$$(2.23) \qquad \rho_1(u, n) = \rho(u, 0) \prod_{m=1}^{n} \frac{F(u)}{m} = \rho(u, 0)\frac{F(u)^n}{n!}.$$

Hence, the corresponding normalized density is a Poisson process with rate $F(u)$

$$(2.24) \qquad \rho_1(u, n) = \mathrm{e}^{-F(u)}\frac{F(u)^n}{n!}.$$

There are two time-scales in the CK equation (2.21), the synaptic time constant τ and the time constant τ_a, which characterizes the relaxation rate of population activity. In the limit $\tau \to 0$ for fixed τ_a, (2.21) reduces to the neural master equation [17, 18, 7] with $\mathbf{u} = \mathbf{u}(\mathbf{n})$ such that $v_\alpha(\mathbf{u}(\mathbf{n}), \mathbf{n}) = 0$. On the other hand, if $\tau_a \to 0$ for fixed τ, then we obtain deterministic voltage or current-based mean-field equations

$$\tau\frac{du_\alpha}{dt} = \langle v_\alpha \rangle(\mathbf{u}(t)) \equiv \sum_{\mathbf{n}} v_\alpha(\mathbf{u}(t), \mathbf{n})\rho(\mathbf{u}(t), \mathbf{n})$$

$$(2.25) \qquad = -u_\alpha(t) + \sum_{\beta=1}^{M} w_{\alpha\beta} \sum_{\mathbf{n}} n_\beta\rho(\mathbf{u}(t), \mathbf{n}).$$

Since $\rho(\mathbf{u}, \mathbf{n})$ is given by the product of independent Poisson processes with rates $F(u_\alpha)$, consistent with the operating regime of the Buice et al. master equation [17, 18], it follows that

$$(2.26) \qquad \langle n_\beta \rangle = F(u_\beta),$$

and (2.25) reduces to the standard voltage or current-based activity equation. Note that the limit $\tau_a \to 0$ is analogous to the slow synapse approximation used by Ermentrout [25] to reduce

deterministic conductance-based neuron models to voltage-based rate models. Now suppose that the network operates in the regime $0 < \tau_a/\tau \equiv \epsilon \ll 1$, for which there are typically a large number of transitions between different firing states $\mathbf{n}$ while the synaptic currents $\mathbf{u}$ hardly change at all. This suggests that the system rapidly converges to the (quasi-)steady-state $\rho(\mathbf{u}, \mathbf{n})$, which will then be perturbed as $\mathbf{u}$ slowly evolves. The resulting perturbations can be analyzed using a quasi-steady-state diffusion or adiabatic approximation, in which the CK equation (2.21) is approximated by an FP equation. This method was first developed from a probabilistic perspective by Papanicolaou [67]; see also [34]. It has subsequently been applied to a wide range of problems in biology, including cell movement [65, 40], traveling-wave-like behavior in models of slow axonal transport [70, 32, 33], and molecular motor-based models of random intermittent search [57, 59, 58, 11]. The diffusion approximation captures the Gaussian-like fluctuations within the basin of attraction of a fixed point of the mean-field equations and can be used to investigate effects such as the noise-induced amplification of subthreshold oscillations (quasicycles) in a manner similar to that of an FP [8]. However, for small ϵ it yields exponentially large errors for the transition rates between metastable states. (A similar problem arises in approximating chemical master equations by an FP equation in the large N limit [39, 24].) Hence, it is necessary to apply an alternative approach based on a WKB approximation and matched asymptotics.

3. Metastable states in a one-population model. In order to develop the basic analytical framework, consider the simple case of a single recurrent population ($M = 1$) evolving according to the CK equation

$$(3.1) \qquad \frac{\partial p}{\partial t} + \frac{\partial [v(u,n)p(u,n,t)]}{\partial u} = \frac{1}{\epsilon} \sum_m A(n,m;u)p(u,m,t)$$

with boundary condition $p(u, -1, t) \equiv 0$, drift term

$$(3.2) \qquad v(u,n) = -u + wn,$$

and tridiagonal transition matrix

$$(3.3) \qquad A(n, n-1; u) = F(u), \quad A(n,n;u) = -F(u) - n, \quad A(n, n+1; u) = n+1.$$

Following the general discussion in section 2.2, we expect the finite-time behavior of the stochastic population to be characterized by small perturbations about the stable steady-state of the underlying jump Markov process, with u treated as a constant over time-scales comparable to the relaxation time of the birth–death process. As shown in section 2.2, the steady-state density is given by a Poisson process,

$$(3.4) \qquad \rho(u,n) = \frac{[F(u)]^n \mathrm{e}^{-F(u)}}{n!},$$

and the mean-field equation obtained in the $\epsilon \to 0$ limit is

$$(3.5) \qquad \frac{du}{dt} = \sum_{n=0}^{\infty} v(u,n)\rho(u,n) = -u + wF(u) \equiv -\frac{d\Psi}{du}.$$
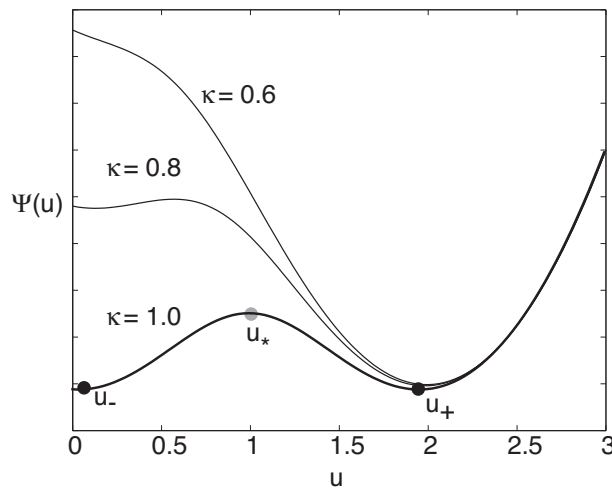
Figure 1. *Bistable potential Ψ for the deterministic network satisfying $\dot{u} = -u + F(u) = -d\Psi/du$ with F given by the sigmoid (2.10) for $\gamma = 4$, $\kappa = 1.0$, $F_0 = 2$. There exist two stable fixed points $u_\pm$ separated by an unstable fixed point u_*. As the threshold κ is reduced the network switches to a monostable regime via a saddle-node bifurcation.*

The sigmoid function $F(u)$ given by (2.10) is a bounded, monotonically increasing function of u with $F(u) \to F_0$ as $u \to \infty$ and $F(u) \to 0$ as $u \to -\infty$. Moreover, $F'(u) = \gamma F_0/[4\cosh^2(\gamma(u-\kappa)/2)]$ so that $F(u)$ has a maximum slope at $u = \kappa$ given by $\gamma F_0/4$. It follows that the function $-u + wF(u)$ only has one zero if $w\gamma F_0 < 4$ and this corresponds to a stable fixed point. On the other hand, if $w\gamma F_0 > 4$, then, for a range of values of the threshold κ, $[\kappa_1, \kappa_2]$, there exists a pair of stable fixed points $u_\pm$ separated by an unstable fixed point u_* (bistability). A stable/unstable pair vanishes via a saddle-node bifurcation at $\kappa = \kappa_1$ and $\kappa = \kappa_2$. This can also be seen graphically by plotting the potential function $\Psi(u)$, whose minima and maxima correspond to stable and unstable fixed points of the mean-field equation. An example of the bistable case is shown in Figure 1.

As highlighted in section 2.2, if the system operates in the regime $0 < \epsilon \ll 1$, there are typically a large number of transitions between different discrete states n, while the synaptic variable u hardly changes at all. This suggests that the system rapidly converges to the (quasi-)steady-state $\rho(u, n)$, which will then be perturbed as u slowly evolves. This motivates carrying out a quasi-steady-state (QSS) diffusion or adiabatic approximation, in which the CK equation (4.1) is approximated by an FP equation. The basic idea of the QSS reduction is to decompose the probability density as

$$(3.6) \qquad p(u, n, t) = C(u, t)\rho(u, n) + \epsilon\Delta(u, n, t),$$

where $\sum_n p(u, n, t) = C(u, t)$ and $\sum_n \Delta(x, n, t) = 0$. Carrying out an asymptotic expansion in ϵ, it can be shown that C evolves according to the FP equation [67, 34, 59]

$$(3.7) \qquad \frac{\partial C}{\partial t} = -\frac{\partial}{\partial x}(\mathcal{F}C) + \epsilon\frac{\partial}{\partial x}\left(\mathcal{D}\frac{\partial C}{\partial x}\right),$$

with the drift term given by

$$(3.8) \qquad \mathcal{F}(u) = \sum_{n=0}^{\infty} v(u,n)\rho(u,n)$$

and diffusion coefficient

$$(3.9) \qquad \mathcal{D}(u) = \sum_{n=0}^{\infty} Z(u,n)v(u,n),$$

where $Z(u,n)$ is the unique solution to

$$(3.10) \qquad \sum_m A(n,m;u)Z(u,m) = [\mathcal{F}(u) - v(u,n)]\rho(u,n)$$

with $\sum_m Z(u,m) = 0$. Note that we have dropped $\mathcal{O}(\epsilon)$ contributions to the drift term; if these were included, then (3.7) would be of the standard Stratonovich form [34]. The FP equation captures the Gaussian-like fluctuations within the basin of attraction of a fixed point of the mean-field equations. However, the problem we wish to address is how to analyze the effects of fluctuations (for $0 < \epsilon \ll 1$) on rare transitions between the metastable states $u_\pm$ of the underlying mean-field equation. As highlighted in section 2.2, it is not possible to use a QSS diffusion approximation, since this yields exponentially large errors in the transition rates. Therefore, we will proceed using the asymptotic methods recently introduced to analyze spontaneous action potentials in a conductance-based single-neuron model with stochastic sodium ion channels [41]. The latter model is described by a CK equation identical in form to (3.1) but with a different drift term and transition matrix. Moreover, u represents membrane voltage and n represents the number of open ion channels. Nevertheless, the basic asymptotic methods developed in [41] can be adapted to the one-population network model.

Suppose that the system starts in the left-hand well of the potential function $\Psi(u)$ (see Figure 1) at the stable state u_-. In order to estimate the transition rate from the left to right well, we place an absorbing boundary at the unstable fixed point u_*. (The subsequent time to travel from u_* to the fixed point u_+ is insignificant and can be neglected.) Thus, the CK equation (3.1) is supplemented by the absorbing boundary conditions

$$(3.11) \qquad p(u_*,n,t) = 0 \quad \text{for } n = 0,\dots,k-1,$$

where $0 < k < \infty$ is the number of firing states for which the drift $v(u_*,n) < 0$. The initial condition is taken to be

$$(3.12) \qquad p(u,n,0) = \delta(u-u_-)\delta_{n,n_0}.$$

Since the drift $v(u,n) = -u + wn > 0$ for all $n \geq 0$ and $u \to 0^+$, it follows that we can set $p(u,n,t) \equiv 0$ for all $u \leq 0$. In other words, we can focus on the domain $u \in [0, u^*]$ in which both the probability and flux vanish at $u = 0$. Let T denote the (stochastic) first passage time for which the system first reaches u_*, given that it started at u_-. The distribution of first passage times is related to the survival probability that the system hasn't yet reached u_*:

$$(3.13) \qquad S(t) \equiv \sum_{n=0}^{\infty} \int_0^{u_*} p(u,n,t)du.$$

That is, $\text{Prob}\{t > T\} = S(t)$ and the first passage time density is

$$(3.14) \qquad f(t) = -\frac{dS}{dt} = -\sum_{n=0}^{\infty} \int_0^{u_*} \frac{\partial p}{\partial t}(u, n, t) du.$$

Substituting for $\partial p/\partial t$ using the CK equation (3.1) shows that

$$(3.15) \qquad f(t) = \sum_{n=0}^{\infty} \int_0^{u_*} \frac{\partial[v(u, n)p(u, n, t)]}{\partial u} du = \sum_{n=0}^{\infty} v(u_*, n)p(u_*, n, t).$$

We have used $\sum_n A(n, m; u) = 0$ and $p(0, n, t) = 0$. The first passage time density can thus be interpreted as the probability flux $J(u_*, t)$ at the absorbing boundary, since we have the conservation law

$$(3.16) \qquad \sum_{n=0}^{\infty} \frac{\partial p(u, n, t)}{\partial t} = -\frac{\partial J(u, t)}{\partial u}, \quad J(u, t) = \sum_{n=0}^{\infty} v(u, n)p(u, n, t).$$

(If the absorbing boundary at $u = u^*$ were replaced by a reflecting boundary, then $J(u^*, t) = 0$ and the probability would be conserved within $[0, u^*]$.)

The first passage time problem in the weak noise limit ($\epsilon \ll 1$) has been well studied in the case of FP equations and master equations; see, for example, [46, 49, 39, 54, 24, 48, 72]. (For an FP equation ϵ would represent the noise amplitude, whereas for a master equation $\epsilon = 1/N$, where N is the number of discrete states.) One of the characteristic features of the weak noise limit is that the flux through the absorbing boundary and the inverse of the mean first passage time $\langle T \rangle$ are exponentially small, that is, $\langle T \rangle \sim e^{-C/\epsilon}$ for some constant C. This means that standard singular perturbation theory cannot be used to solve the resulting boundary value problem, in which one matches inner and outer solutions of a boundary layer around the point $u = u_*$. Instead, one proceeds by finding a quasistationary solution using a Wentzel–Kramers–Brillouin (WKB) approximation. Recently, this approach has been extended by Newby and Keener [61] to a CK equation of the form (3.1), arising from a model of stochastic ion channels, using a so-called projection method [83]. We will proceed by developing this analysis for the general CK equation (3.1) on the domain $u \in [0, u_*]$, assuming that A and v are defined so that there exists a unique stationary density $\rho(u, n)$, the deterministic potential $\Psi(u)$ of the mean-field equation $\dot{u} \equiv \mathcal{F}(u) = \sum_{n=0}^{\infty} \rho(u, n)v(u, n)$ is bistable (see Figure 1), and the probability flux is always positive in a neighborhood of $u = 0$. We then apply the general results to the particular neural population model.

3.1. Quasistationary approximation and the projection method. In order to apply the projection method, it is necessary to assume certain properties of the non-self-adjoint linear operator $-\widehat{L}$ on the right-hand side of (3.1) with respect to the Hilbert space of functions $h : [0, u_*] \times \mathbf{Z}^+ \to \mathbb{R}$ with inner product defined according to

$$(3.17) \qquad \langle h, g \rangle = \sum_{n=0}^{\infty} \int_0^{u_*} h(u, n)g(u, n) du.$$

(i) $\widehat{L}$ has a complete set of eigenfunctions ϕ_r with

$$(3.18) \qquad \widehat{L}\phi_r(u,n) \equiv \frac{d}{du}(v(u,n)\phi_r(u,n)) - \frac{1}{\epsilon}\sum_{m=0}^{\infty} A(n,m;u)\phi_r(u,m) = \lambda_r \phi_r(u,n),$$

together with the boundary conditions

$$(3.19) \qquad \phi_r(u_*,n) = 0 \quad \text{for } n = 0,\ldots,k-1.$$

(ii) The eigenvalues λ_r all have positive definite real parts and the smallest eigenvalue λ_0 is real and simple. Thus we can introduce the ordering $0 < \lambda_0 < \mathrm{Re}[\lambda_1] \leq \mathrm{Re}[\lambda_2] \leq \cdots$.

(iii) λ_0 is exponentially small, $\lambda_0 \sim \mathrm{e}^{-C/\epsilon}$, whereas $\mathrm{Re}[\lambda_r] = \mathcal{O}(1)$ for $r \geq 1$. In particular, $\lim_{\epsilon \to 0} \lambda_0 = 0$ and $\lim_{\epsilon \to 0} \phi_0(u,n) = \rho(u,n)$.

Under the above assumptions, we can introduce the eigenfunction expansion

$$(3.20) \qquad p(u,n,t) = \sum_{r=0}^{\infty} C_r \mathrm{e}^{-\lambda_r t}\phi_r(u,n),$$

with $\lambda_0 \ll \mathrm{Re}[\lambda_r]$ for all $r \geq 1$. Thus, at large times we have the quasistationary approximation

$$(3.21) \qquad p(u,n,t) \sim C_0 \mathrm{e}^{-\lambda_0 t}\phi_0(u,n).$$

Substituting such an approximation into (3.15) gives

$$(3.22) \qquad f(t) \sim C_0 \mathrm{e}^{-\lambda_0 t}\sum_{n=0}^{\infty} v(u_*,n)\phi_0(u_*,n), \quad \lambda_1 t \gg 1.$$

Equation (3.18) implies that

$$\sum_{n=0}^{\infty}\int_0^{u_*} \widehat{L}\phi_0(u,n)du \equiv \sum_{n=0}^{\infty} v(u_*,n)\phi_0(u_*,n,t)$$

$$= \lambda_0 \sum_{n=0}^{\infty}\phi_0(u,n)du.$$

In other words,

$$(3.23) \qquad \lambda_0 = \frac{\sum_{n=0}^{\infty} v(u_*,n)\phi_0(u_*,n)}{\langle 1,\phi_0\rangle}.$$

Combining equations (3.23) and the quasistationary approximation (3.22) shows that the (normalized) first passage time density reduces to

$$(3.24) \qquad f(t) \sim \lambda_0 \mathrm{e}^{-\lambda_0 t}$$

and, hence, $\langle T\rangle = \int_0^{\infty} tf(t)dt \sim 1/\lambda_0$.

It remains to obtain an approximation ϕ_ϵ of the principal eigenfunction ϕ_0, which can be achieved using the WKB method as described in section 3.2. This yields a quasistationary density that approximates ϕ_0 up to exponentially small terms at the boundary, that is,

$$(3.25) \qquad \widehat{L}\phi_\epsilon = 0, \quad \phi_\epsilon(u_*, n) = \mathcal{O}(\mathrm{e}^{-C/\epsilon}).$$

In order to express λ_0 in terms of the quasistationary density ϕ_ϵ, we consider the eigenfunctions of the adjoint operator, which satisfy the equation

$$(3.26) \qquad \widehat{L}^*\xi_s(u, n) \equiv v(u, n)\frac{d\xi_s(u, n)}{du} - \frac{1}{\epsilon}\sum_m A(m, n; u)\xi_s(u, m) = \lambda_s\xi_s(u, n)$$

and the boundary conditions

$$(3.27) \qquad \xi_s(u_*, n) = 0, \quad n \geq k.$$

Given our assumptions regarding the spectral properties of $\widehat{L}$, the two sets of eigenfunctions form a biorthonormal set with

$$(3.28) \qquad \langle \phi_r, \xi_s \rangle = \delta_{r,s}.$$

Now consider the identity

$$(3.29) \qquad \langle \phi_\epsilon, \widehat{L}^*\xi_0 \rangle = \lambda_0 \langle \phi_\epsilon, \xi_0 \rangle.$$

Integrating by parts the left-hand side of (3.29) picks up a boundary term so that

$$(3.30) \qquad \lambda_0 = -\frac{\sum_{n=0}^{\infty} \phi_\epsilon(u_*, n)v(u_*, n)\xi_0(u_*, n)}{\langle \phi_\epsilon, \xi_0 \rangle}.$$

The calculation of the principal eigenvalue λ_0 thus reduces to the problem of determining the quasistationary density ϕ_ϵ and the adjoint eigenfunction ξ_0 using perturbation methods (see below). Once λ_0 has been evaluated, we can then identify the mean first passage time $\langle T \rangle$ with λ_0^{-1}.

3.2. WKB method and the quasistationary density. We now use the WKB method [39, 54, 24, 48, 72] to compute the quasistationary density ϕ_ϵ. We seek a solution of the form

$$(3.31) \qquad \phi_\epsilon(u, n) \sim R(u, n)\exp\left(-\frac{\Phi(u)}{\epsilon}\right),$$

where $\Phi(u)$ is a scalar potential. Substituting into the equation $\widehat{L}\phi_\epsilon = 0$ gives

$$(3.32) \qquad \sum_{m=0}^{\infty}\left(A(n, m; u) + \Phi'(u)\delta_{n,m}v(u, m)\right)R(u, m) = \epsilon\frac{dv(u, n)R(u, n)}{du},$$

where $\Phi' = d\Phi/du$. Introducing the asymptotic expansions $R \sim R^{(0)} + \epsilon R^{(1)}$ and $\Phi \sim \Phi_0 + \epsilon\Phi_1$, the leading-order equation is

$$(3.33) \qquad \sum_{m=0}^{\infty} A(n, m; u)R^{(0)}(u, m) = -\Phi_0'(u)v(u, n)R^{(0)}(u, n).$$

(Note that since $v(u, n)$ is nonzero almost everywhere for $u \in [0, u_*]$, we can identify $-\Phi_0'$ and $R^{(0)}$ as an eigenpair of the matrix operator $\widehat{A}(n, m; u) = A(n, m; u)/v(u, n)$ for fixed u.) Positivity of the probability density ϕ_ϵ requires positivity of the corresponding solution $R^{(0)}$. One positive solution is $R^{(0)} = \rho$, for which $\Phi_0' = 0$. However, such a solution is not admissible since $\Phi_0 = $ constant. It can be proven using linear algebra (see Theorem 3.1 of [41]) that since $v(u, n)$ for fixed $u \in [0, u_*]$ changes sign as n increases from zero, then there exists one other positive solution, such that $\Phi_0'(u)$ has the correct sign and vanishes at the fixed points. Hence, it can be identified as the appropriate WKB solution.

Proceeding to the next order in the asymptotic expansion of (3.32),

$$\sum_{m=0}^{\infty} \left(A(n, m; u) + \Phi_0'(u)\delta_{n,m}v(u, m) \right) R^{(1)}(u, m)$$

(3.34)
$$= \frac{d[v(u, n)R^{(0)}(u, n)]}{du} - \Phi_1'(u)v(u, n)R^{(0)}(u, n).$$

For fixed u, the matrix operator

(3.35)
$$\bar{A}(n, m; u) = A(n, m; u) + \Phi_0'(u)\delta_{n,m}v(u, m)$$

on the left-hand side of this equation has a one-dimensional null space spanned by the positive WKB solution $R^{(0)}$. The Fredholm alternative theorem then implies that the right-hand side of (3.34) is orthogonal to the left null vector S of $\bar{A}$. That is, we have the solvability condition

(3.36)
$$\sum_{n \in I} S(u, n) \left[\frac{dv(u, n)R^{(0)}(u, n)}{du} - \Phi_1'(u)v(u, n)R^{(0)}(u, n) \right] = 0,$$

with S satisfying

(3.37)
$$\sum_{n=0}^{\infty} S(u, n) \left(A(n, m; u) + \Phi_0'(u)\delta_{n,m}v(u, m) \right) = 0.$$

Given $R^{(0)}, S$, and Φ_0, the solvability condition yields the following equation for Φ_1:

(3.38)
$$\Phi_1'(u) = \frac{\sum_{n=0}^{\infty} S(u, n)[v(u, n)R^{(0)}(u, n)]'}{\sum_{n=0}^{\infty} S(u, n)v(u, n)R^{(0)}(u, n)}.$$

Combining the various results, and defining

(3.39)
$$k(u) = \exp\left(-\int_{u_-}^{u_*} \Phi_1'(y)dy \right),$$

gives to leading order in ϵ

(3.40)
$$\phi_\epsilon(u, n) \sim \mathcal{N}k(u) \exp\left(-\frac{\Phi_0(u)}{\epsilon} \right) R^{(0)}(u, n),$$

where we choose $\sum_n R^{(0)}(u, n) = 1$ for all u and $\mathcal{N}$ is the normalization factor,

$$(3.41) \qquad \mathcal{N} = \left[\int_0^{u_*} k(u) \exp\left(-\frac{\Phi_0(u)}{\epsilon} \right) \right]^{-1}.$$

The latter can be approximated using Laplace's method to give

$$(3.42) \qquad \mathcal{N} \sim \frac{1}{k(u_-)} \sqrt{\frac{|\Phi_0''(u_-)|}{2\pi\epsilon}} \exp\left(\frac{\Phi_0(u_-)}{\epsilon} \right).$$

3.3. Perturbation analysis of the adjoint eigenfunction. Following [61, 41, 55], the adjoint eigenfunction $\xi_0(u, n)$ can be approximated using singular perturbation methods. Since λ_0 is exponentially small in ϵ, (3.26) yields the leading-order equation

$$(3.43) \qquad \epsilon v(u, n) \frac{d\xi_0(u, n)}{du} + \sum_{m=0}^{\infty} A(m, n; u) \xi_0(u, m) = 0,$$

supplemented by the absorbing boundary condition

$$(3.44) \qquad \xi_0(u_*, n) = 0, \quad n \geq k.$$

A first attempt at obtaining an approximate solution that also satisfies the boundary conditions is to construct a boundary layer in a neighborhood of the unstable fixed point u_* by performing the change of variables $u = u_* - \epsilon z$ and setting $Q(z, n) = \xi_0(u_* - \epsilon z)$. Equation (3.43) then becomes

$$(3.45) \qquad v(u_*, n) \frac{dQ(z, n)}{dz} + \sum_{m=0}^{\infty} A(m, n; u_*) Q(z, m) = 0.$$

This inner solution has to be matched with the outer solution $\xi_0(u, n) = 1$, which means that

$$(3.46) \qquad \lim_{z \to \infty} Q(z, n) = 1$$

for all n. Consider the eigenvalue equation

$$(3.47) \qquad \sum_{n=0}^{\infty} \left(A(n, m; u) - \mu_r(u) \delta_{n,m} v(u, m) \right) S_r(u, n) = 0.$$

We take $S_0(u, n) = 1$ so that $\mu_0 = 0$ and set $S_1(u, n) = S(u, n), \mu_1(u) = -\Phi_0'(u)$, where S satisfies (3.37). We then introduce the eigenfunction expansion

$$(3.48) \qquad Q(z, n) = c_0 + \sum_{r=1}^{\infty} c_r S_r(u_*, n) e^{-\mu_r(u_*)z}.$$

In order that the solution remains bounded as $z \to \infty$ we require that $c_r = 0$ if $\mathrm{Re}[\mu_r(u_*)] < 0$. The boundary conditions (3.44) generate a system of linear equations for the coefficients c_r

with codimension k. One of the unknowns is determined by matching the outer solution, which suggests that there are $k-1$ eigenvalues with negative real part. We will set the corresponding coefficients to zero so that the sum over r in (3.48) only contains terms that decay to zero as $z \to \infty$.

There is, however, one problem with the above eigenfunction expansion, namely, that $\mu_1(u_*) = 0$ so that the zero eigenvalue is degenerate. (The vanishing of $\mu_1 = -\Phi_0'$ at fixed points follows from Theorem 3.1 of [41].) Hence, the solution needs to include a secular term involving the generalized eigenvector $\widehat{S}$,

$$(3.49) \qquad \sum_{n=0}^{\infty} A(n, m; u_*)\widehat{S}(u_*, n) = -v(u_*, m).$$

The Fredholm alternative theorem ensures that $\widehat{S}$ exists and is unique, since the stationary density $\rho(u_*, m)$ is the right null vector of $A(n, m; u_*)$, and

$$\sum_{n=0}^{\infty} \rho(u_*, n)v(u_*, n) \equiv \mathcal{F}(u_*) = 0.$$

The solution for $Q(z, n)$ is now

$$(3.50) \qquad Q(z, n) = c_0 + c_1(\widehat{S}(u_*, n) - z) + \sum_{r \geq 2} c_r S_r(u_*, n)\mathrm{e}^{-\mu_r(u_*)z}.$$

The presence of the secular term means that the solution is unbounded in the limit $z \to \infty$, which means that the inner solution cannot be matched with the outer solution. One way to remedy this situation is to introduce an alternative scaling in the boundary layer of the form $u = u_* - \epsilon^{1/2}z$, as detailed in [55]. One can then eliminate the secular term $-c_1 z$ and show that

$$(3.51) \qquad c_1 \sim \sqrt{\frac{2|\Phi_0''(u_*)|}{\pi}} + \mathcal{O}(\epsilon^{1/2}), \qquad c_r = \mathcal{O}(\epsilon^{1/2}) \quad \text{for } r \geq 2$$

It turns out that we require only the first coefficient c_1 in order to evaluate the principal eigenvalue λ_0 using (3.30). This follows from (3.33) and (3.47), and the observation that the left and right eigenvectors of the matrix $\widehat{A}(n, m; u) = A(n, m; u)/v(u, n)$ are biorthogonal. In particular, since the quasistationary approximation ϕ_ϵ is proportional to $R^{(0)}$ (see (3.40)), it follows that ϕ_ϵ is orthogonal to all eigenvectors S_r, $r \neq 1$. Simplifying the denominator of (3.30) by using the outer solution $\xi_0 \sim 1$, we obtain

$$\lambda_0 \sim -\frac{\sum_{n=0}^{\infty} \xi_0(u_*, n)v(u_*, n)\phi_\epsilon(u_*, n)}{\langle \phi_\epsilon, 1 \rangle}$$

$$(3.52) \qquad \sim c_1 \frac{k(u_*)B(u_*)}{k(u_-)} \sqrt{\frac{|\Phi''(u_-)|}{2\pi}} \exp\left(-\frac{\Phi_0(u_*) - \Phi_0(u_-)}{\epsilon}\right),$$

with

$$(3.53) \qquad B(u_*) = -\sum_{n=1}^{\infty} \widehat{S}(u_*, n) v(u_*, n) \rho(u_*, n).$$

Substituting for c_1,

$$(3.54) \qquad \lambda_0 \sim \frac{1}{\pi} \frac{k(u_*)B(u_*)}{k(u_-)} \sqrt{\Phi_0''(u_-)|\Phi_0''(u_*)|} \exp\left(-\frac{\Phi_0(u_*) - \Phi_0(u_-)}{\epsilon}\right).$$

Finally, comparison of (3.49) and (3.53) with (3.10) and (3.9) establishes that $B(u_*) \equiv \mathcal{D}(u_*)$.

3.4. Calculation of principal eigenvalue. We now apply the general analysis presented in sections 3.1 and 3.2 to the particular example of a stochastic neural population with v and A defined by (3.2) and (3.3). There are three basic steps needed in order to evaluate the principal eigenvalue (3.54).

(1) Find the unique nontrivial positive eigenfunction $\psi_n(u) = R^{(0)}(u, n)$ and associated eigenvalue $\mu(u) = -\Phi_0'(u)$. In the case of the neural population model, (3.33) takes the explicit form

$$(3.55) \qquad F(u)\psi_{n-1}(u) - (F(u) + n)\psi_n(u) + (n+1)\psi_{n+1}(u) = \mu(-u + wn)\psi_n(u).$$

Trying a solution for ψ of the form

$$(3.56) \qquad \psi_n(u) = \frac{\Lambda(u)^n}{n!}$$

yields the following equation relating Λ and the corresponding eigenvalue μ:

$$\left[\frac{F(u)}{\Lambda} - 1\right] n + \Lambda - F(u) = \mu(u)(-u + wn).$$

We now collect terms independent of n and linear in n, respectively, to obtain the pair of equations

$$\mu = \frac{1}{w}\left[\frac{F(u)}{\Lambda} - 1\right], \quad \Lambda = F(u) - \mu u.$$

We deduce that

$$(3.57) \qquad \Lambda = \frac{u}{w}, \quad \mu = \frac{1}{w}\left[\frac{wF(u)}{u} - 1\right],$$

and the normalized eigenfunction is

$$(3.58) \qquad \psi_n(u) = \frac{1}{n!}\left(\frac{u}{w}\right)^n e^{-u/w}.$$

Note that $\mu(u)$ vanishes at the fixed points u_-, u_* of the mean-field equation (3.5) with $\mu(u) > 0$ for $0 < u < u_-$ and $\mu(u) < 0$ for $u_- < u < u_*$. Moreover, comparing (3.4) with (3.58)

establishes that $\psi_n(u) = \rho(u, n)$ at the fixed points $u_*, u_\pm$. In conclusion $R^{(0)}(u, n) = \psi_n(u)$ and the effective potential Φ_0 is given by

$$(3.59) \qquad \Phi_0(u) = -\int_{u_-}^{u^*} \mu(y) dy.$$

The effective potential is defined up to an arbitrary constant, which has been fixed by setting $\Phi_0(u_-) = 0$.

(2) Determine the null eigenfunction $\eta_n(u) = S(u, n)$ of (3.37), which becomes

$$(3.60) \qquad F(u)\eta_{m+1} - (F(u) + m)\eta_m + m\eta_{m-1} = \mu(u)[-u + mw]\eta_m.$$

Trying a solution of the form $\eta_m = \Gamma^m$ yields

$$(3.61) \qquad (F(u))\Gamma - (F(u) + m) + m\Gamma^{-1} = \mu(u)[-u + mw].$$

Γ is then determined by canceling terms linear in m, which finally gives

$$(3.62) \qquad \eta_n(u) = \left(\frac{u}{wF(u)}\right)^n.$$

(3) Calculate the generalized eigenvector $\zeta_n = \widehat{S}(u_*, n)$ of (3.49), which reduces to

$$(3.63) \qquad F(u_*)\zeta_{n+1} + n\zeta_{n-1} - (F(u_*) + n)\zeta_n = u_* - wn.$$

It is straightforward to show that this has the solution (up to an arbitrary constant that doesn't contribute to the principal eigenvalue)

$$(3.64) \qquad \zeta_n = wn.$$

It follows from (3.4) and (3.64) that the factor $B(u_*)$ defined by (3.53) is

$$B(u_*) = w\sum_{n=0}^{\infty} \rho(u_*, n)\left[-u_* n + wn^2\right]$$
$$(3.65) \qquad \qquad = w\left[-u_*\langle n\rangle + w\langle n^2\rangle\right].$$

Recall that $\rho(u, n)$ is given by a Poisson density with rate $F(u)$, which implies that $\langle n^2\rangle = \langle n\rangle + \langle n\rangle^2$ with $\langle n\rangle = F(u)$. Therefore,

$$(3.66) \qquad B(u_*) = wF(u_*)\left[2wF(u_*) - u_*\right],$$

which reduces to $B(u_*) = w^2 F(u_*)^2$ since $u^* = wF(u^*)$ at a fixed point.

It is instructive to compare the effective potential Φ_0 obtained using the WKB approximation with the potential obtained using the FP equation (3.7) based on the QSS approximation. First, substitute (3.4), (3.2), and (3.3) into (3.9) and (3.10). We find that $Z(u, n) = wn\rho(u, n)$ so that

$$(3.67) \qquad \mathcal{D}(u) = w[-u\langle n\rangle + w\langle n^2\rangle] = B(u).$$
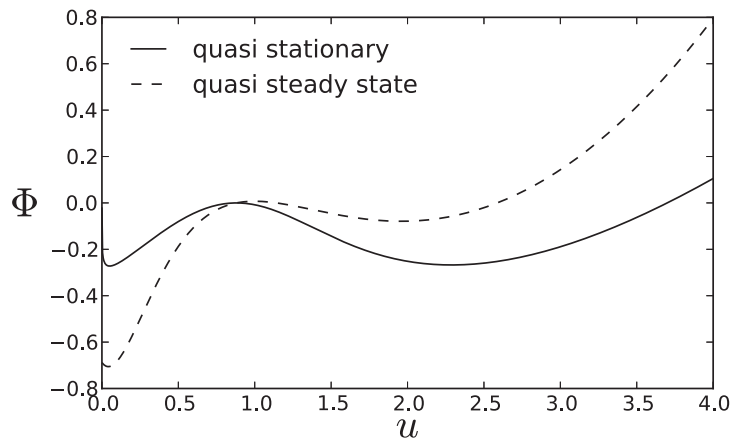
Figure 2. *Comparison of the double-well potentials $\Phi_0(u)$ and $\widehat{\Phi}_0(u)$ obtained using the quasistationary approximation and the QSS diffusion approximation, respectively. Parameter values are chosen so that deterministic network is bistable: $F_0 = 2$, $\gamma = 4$, $\kappa = 1$, and $w = 1.15$.*

The steady-state solution of the FP equation (3.7) takes the form $C(u) \sim \exp^{-\widehat{\Phi}_0(u)/\epsilon}$ with stochastic potential

$$(3.68) \qquad \widehat{\Phi}_0(u) = -\int^u \frac{\mathcal{F}(y)}{\mathcal{D}(y)} dy = -\int^u \frac{-y + wF(y)}{wF(y)[2wF(y) - y]} dy.$$

Note that $\widehat{\Phi}_0$ differs from the potential Φ_0, (3.59), obtained using the more accurate WKB method. Equations (3.57) and (3.59) show that the latter has the integral form

$$(3.69) \qquad \Phi_0(u) = -\int^u \frac{1}{w} \left[\frac{wF(y)}{y} - 1 \right] dy.$$

Thus, there will be exponentially large differences between the steady-states for small ϵ. However, it gives the same Gaussian-like behavior close to a fixed point u_*, that is,

$$(3.70) \qquad \left. \frac{\partial \Phi_0}{\partial u} \right|_{u=u_*} = \left. \frac{\partial \widehat{\Phi}_0}{\partial u} \right|_{u=u_*} = 0, \quad \left. \frac{\partial^2 \Phi_0}{\partial u^2} \right|_{u=u_*} = \left. \frac{\partial^2 \widehat{\Phi}_0}{\partial u^2} \right|_{u=u_*} = \left. \frac{1 - wF'(u)}{wu} \right|_{u=u_*}.$$

3.5. Numerical results. In Figure 2, we plot the potential function Φ_0 of (3.69), which is obtained using the quasistationary approximation in a parameter regime for which the underlying deterministic network is bistable. We also plot the corresponding potential function $\widehat{\Phi}_0$ of (3.68) under the QSS diffusion approximation. The differences between the two lead to exponentially large differences in estimates for the mean exit times when ϵ is small. The mean exit time from the left and right wells is shown in Figure 3. Solid curves show the analytical approximation $T \sim 1/\lambda_0$, where λ_0 is given by (3.52), as a function of $1/\epsilon$. For comparison, the mean exit time computed from averaged Monte Carlo simulations of the full stochastic system are shown as symbols. (Details of the simulations are given in section 4.6.) From
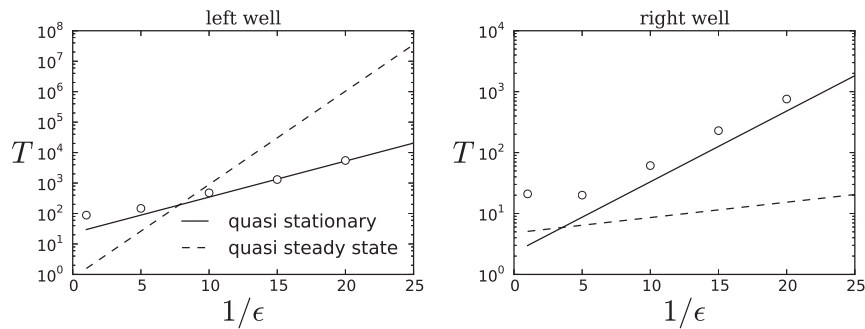
Figure 3. *Mean exit time from the left and right wells calculated using the quasistationary approximation (solid line) and the QSS diffusion approximation (dashed line). The open circles represent data points obtained by numerically solving the corresponding jump velocity Markov process using the Gillespie algorithm. Parameter values are the same as in Figure* 2.

(3.52), we expect the log of the mean exit time to be an asymptotically linear function of $1/\epsilon$, and this is confirmed by Monte Carlo simulations. The slope is determined by the depth of the potential well, and the vertical shift is determined by the prefactor. Also shown is the corresponding mean first passage time calculated using the QSS diffusion approximation (dashed lines), which is typically several orders of magnitude out, and validates the relative accuracy of the quasistationary approximation.

4. Metastable states in a two-population model. The same basic analytical steps as section 3 can also be used to study multipopulation models ($M > 1$). One now has M piecewise-deterministic variables U_α and M discrete stochastic variables N_α evolving according to the CK equation (2.19). The mean first passage time is again determined by the principal eigenvalue λ_0 of the corresponding linear operator. As in the one-population model, λ_0 can be expressed in terms of inner products involving a quasistationary density ϕ_ϵ, obtained using a multidimensional WKB method, and the principal eigenvector ξ_0 of the adjoint linear operator, calculated using singular perturbation theory. One of the major differences between the one-population model and multidimensional versions is that the latter exhibit much richer dynamics in the mean-field limit, including oscillatory solutions. For example, consider a two-population model ($M = 2$) consisting of an excitatory population interacting with an inhibitory population as shown in Figure 4. This is one of the simplest deterministic networks known to generate limit cycle oscillations at the population level [5] and figures as a basic module in many population models. For example, studies of stimulus-induced oscillations and synchrony in primary visual cortex often take the basic oscillatory unit to be an E-I (excitatory and inhibitory) network operating in a limit cycle regime [73, 37]. Here the E-I network represents a cortical column, which can synchronize with other cortical columns either via long-range synaptic coupling or via a common external drive. In this paper, we will focus on parameter regimes where the two-population model exhibits bistability.

Let $u_1 = x$ and $u_2 = y$ denote the synaptic variables of the excitatory and inhibitory networks, respectively, and denote the corresponding spiking variables by n_x and n_y. The CK
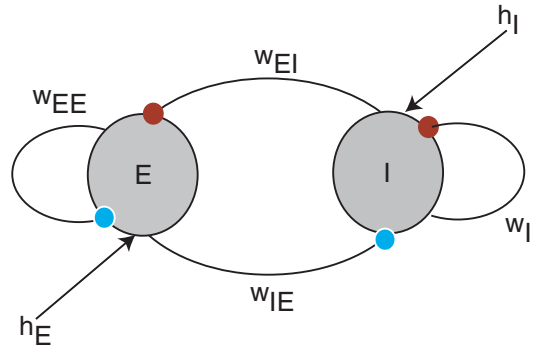
Figure 4. *Two-population E-I network with both intrasynaptic connections w_{EE}, w_{II} and intersynaptic connections w_{IE}, w_{EI}. There could also be external inputs h_E, h_I, which can be incorporated into the rate functions of the two populations by shifting the firing threshold κ.*

equation (2.19) can be written out fully as

$$(4.1) \quad \frac{\partial p}{\partial t} = -\frac{\partial(vp)}{\partial x} - \frac{\partial(\widetilde{v}p)}{\partial y}$$
$$+\frac{1}{\epsilon}\left[\omega_-(n_x+1)p(x,y,n_x+1,n_y,t) + \omega_-(n_y+1)p(x,y,n_x,n_y+1,t)\right]$$
$$+\frac{1}{\epsilon}\left[\omega_+(x)p(x,y,n_x-1,n_y,t) + \omega_+(y)p(x,y,n_x,n_y-1,t)\right]$$
$$-\frac{1}{\epsilon}\left[\omega_-(n_x) + \omega_-(n_y) + \omega_+(x) + \omega_+(y)\right]p(x,y,n_x,n_y,t),$$

where

$$(4.2) \quad v(x,n_x,n_y) = -x + \left[w_{EE}n_x - w_{EI}n_y\right],$$
$$(4.3) \quad \widetilde{v}(y,n_x,n_y) = -y + \left[w_{IE}n_x - w_{II}n_y\right],$$

and

$$(4.4) \quad \omega_+(x) = F(x), \quad \omega_-(n) = n.$$

Thus the synaptic coupling between populations occurs via the drift terms $v, \widetilde{v}$. As in the case of the one-population model, we expect the finite-time behavior to be characterized by small Gaussian fluctuations about the stable steady-state of the corresponding pure birth–death process. We now show that in the limit $N \to \infty$ and $\Delta\tau \to 0$ with $N\Delta t = 1$ and ϵ fixed, the steady-state distribution reduces to a multivariate Poisson process. First, introduce the generating function (for fixed (x,y))

$$(4.5) \quad G(r,s) = \sum_{n_y=0}^{\infty}\sum_{n_y=0}^{\infty} r^{n_x}s^{n_y}p(x,y,n_x,n_y).$$

Setting all derivatives in (4.1) to zero, multiplying both sides by r^{n_x} and s^{n_y}, and summing over n_x, n_y gives the quasilinear equation

$$(4.6) \qquad 0 = (1 - r)\frac{\partial G}{\partial r} + (1 - s)\frac{\partial G}{\partial s} + [(r-1)\omega_+(x) + (s-1)\omega_+(y)]G.$$

This can be solved using the method of characteristics to give

$$(4.7) \qquad G(r, s) = \exp\left([r-1]\omega_+(x) + [s-1]\omega_+(y)\right),$$

which is the generating function for the steady-state Poisson distribution

$$(4.8) \qquad \rho(x, y, n_x, n_y) = \frac{\omega_+(x)^{n_x} e^{-\omega_+(x)}}{n_x!} \cdot \frac{\omega_+(y)^{n_y} e^{-\omega_+(y)}}{n_y!}.$$

Since $\langle n_x \rangle = \omega_+(x), \langle n_y \rangle = \omega_-(y)$, it immediately follows that in the limit $\epsilon \to 0$, we obtain the standard voltage-based mean-field equations for an E-I system:

$$(4.9) \qquad \frac{dx}{dt} = -x + w_{EE}F(x) - w_{EI}F(y),$$

$$(4.10) \qquad \frac{dy}{dt} = -y + w_{IE}F(x) - w_{II}F(y).$$

It is well known that the dynamical system (4.9) exhibits multistability and limit cycle oscillations [5]. We will assume that it is operating in a parameter regime for which there is bistability, as illustrated in Figure 5. For example, if $w_{EE} - w_{EI} = w_{IE} - w_{II} = w$, then $x = y$ is an invariant manifold on which x evolves according to the one-population equation (3.5). Varying the threshold κ then leads to a pitchfork bifurcation and the emergence of bistability.
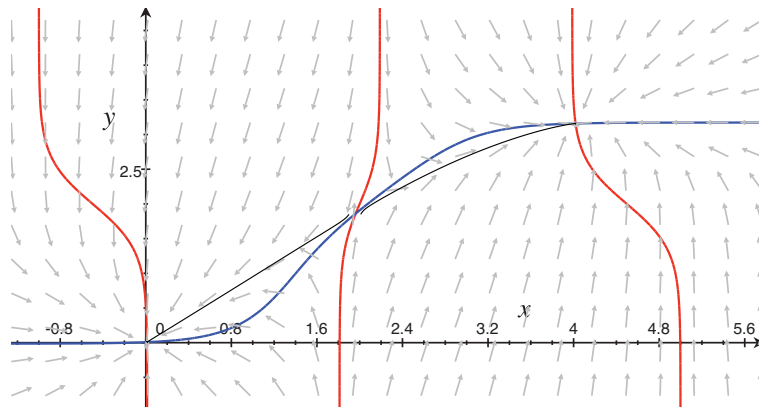
Figure 5. *Deterministic limit of the two-population model, showing bistability. Red curves show the x-nullclines, and the blue curve show the y-nullcline. The red nullcline through the saddle is its stable manifold and acts as the separatrix Σ between the two stable fixed points. Two deterministic trajectories are shown (black curves), starting from either side of the unstable saddle and ending at a stable fixed point. Parameter values are $F_0 = 1$, $\gamma = 3$, $\kappa = 2$, $w_{EE} = 5$, $w_{EI} = 1$, $w_{IE} = 9$, and $w_{II} = 6$.*

In order to analyze the effects of fluctuations for $0 < \epsilon \ll 1$, we rewrite (4.1) in the more compact form

$$(4.11) \qquad \frac{\partial p}{\partial t} = -\frac{\partial}{\partial x}(vp) - \frac{\partial}{\partial y}(\widetilde{v}p) + \frac{1}{\epsilon}\sum_{\mathbf{m}} A(\mathbf{n}, \mathbf{m}; \mathbf{x})p(\mathbf{x}, \mathbf{n}),$$

where $\mathbf{x} = (x, y)$, $\mathbf{n} = (n_x, n_y)$, and the 2-tensor A has the nonzero components

$$(4.12) \qquad A(n_x, n_y, n_x - 1, n_y; \mathbf{x}) = F(x), \quad A(n_x, n_y, n_x, n_y - 1; \mathbf{x}) = F(y),$$

$$(4.13) \qquad A(n_x, n_y, n_x + 1, n_y; \mathbf{x}) = n_x + 1, \quad A(n_x, n_y, n_x, n_y + 1; \mathbf{x}) = n_y + 1,$$

and

$$(4.14) \qquad A(n_x, n_y, n_x, n_y; \mathbf{x}) = -[F(x) + F(y) + n_x + n_y].$$

As in the one-population model, we can restrict the domain of the stochastic dynamics in the (x, y)-plane. In order to show this, multiply both sides of (4.2) and (4.3) by w_{II} and w_{EI}, respectively, and add the resulting equations. Setting

$$(4.15) \qquad \hat{x} = [w_{II}x - w_{EI}y]/\det[\mathbf{w}],$$

with $\det[\mathbf{w}] = w_{EE}w_{II} - w_{EI}w_{IE}$, we have the transformed drift term

$$(4.16) \qquad \hat{v}(\hat{x}, n_x) = -\hat{x} + n_x.$$

Similarly, multiplying both sides of (4.2) and (4.3) by w_{IE} and w_{EE}, respectively, and adding the resulting equations yields

$$(4.17) \qquad \hat{\widetilde{v}}(\hat{y}, n_y) = -\hat{y} + n_y,$$

with

$$(4.18) \qquad \hat{y} = [w_{IE}x - w_{EE}y]/\det[\mathbf{w}].$$

It follows that the dynamics can be restricted to the domain $\hat{x} > 0, \hat{y} > 0$.

4.1. Quasistationary approximation. In order to investigate rare transitions between the metastable states shown in Figure 5, we introduce an absorbing boundary along the separatrix $\mathcal{M}$ separating the two states:

$$(4.19) \qquad p(\mathbf{x}, \mathbf{n}, t) = 0, \quad \mathbf{x} \in \Sigma, \quad \mathbf{n} \in \mathcal{M},$$

with $\mathcal{M}$ the set of integers (n_x, n_y) for which

$$(4.20) \qquad (v(x, n_x, n_y), \widetilde{v}(y, n_x, n_y)) \cdot \widehat{\mathbf{s}} < 0,$$

where $\hat{\mathbf{s}}$ is the unit normal of Σ pointing out of the domain $\mathcal{D}$ of the initial metastable state, which we take to be (x_-, y_-). Following identical arguments to the one-population model, we assume that the probability density has an eigenfunction expansion of the form

$$(4.21) \qquad p(\mathbf{x}, \mathbf{n}, t) = \sum_{r=0}^{\infty} c_r \phi_r(\mathbf{x}, \mathbf{n})e^{-\lambda_r t},$$

with (λ_r, ϕ_r) determined from the eigenvalue equation

$$(4.22) \qquad \widehat{L}\phi_r(\mathbf{x}, \mathbf{n}) \equiv \frac{\partial}{\partial x}(v\phi_r) + \frac{\partial}{\partial y}(\widetilde{v}\phi_r) - \frac{1}{\epsilon}\sum_{\mathbf{m}} A(\mathbf{n}, \mathbf{m}; \mathbf{x})\phi_r(\mathbf{x}, \mathbf{m}) = \lambda_r \phi_r(\mathbf{x}, \mathbf{n}),$$

together with the boundary conditions

$$(4.23) \qquad\qquad \phi_r(\mathbf{x}, \mathbf{n}) = 0, \quad \mathbf{x} \in \Sigma, \quad \mathbf{n} \in \mathcal{M}.$$

We assume that the spectrum of the linear operator (4.22) satisfies the multidimensional version of conditions (i)–(iii) of section 3.1. The principal eigenvalue λ_0 then determines the first passage time density according to $f(t) \sim \lambda_0 e^{-\lambda_0 t}$.

As in the one-population model, the principal eigenvalue λ_0 can be approximated using a spectral projection method that makes use of the adjoint eigenvalue equation

$$\widehat{L}^*\xi_s(\mathbf{x}, \mathbf{n}) \equiv -v(\mathbf{x}, \mathbf{n})\frac{\partial \phi_s(\mathbf{x}, \mathbf{n})}{\partial x} - \widetilde{v}(\mathbf{x}, \mathbf{n})\frac{\partial \phi_s(\mathbf{x}, \mathbf{n})}{\partial y} + \frac{1}{\epsilon}\sum_{\mathbf{m}} A(\mathbf{m}, \mathbf{n}; \mathbf{x})\xi_s(\mathbf{x}, \mathbf{m})$$

$$(4.24) \qquad\qquad = \lambda_s \xi_s(\mathbf{x}, \mathbf{n}),$$

with $\langle \phi_r, \xi_s \rangle = \delta_{r,s}$ and the inner product

$$(4.25) \qquad\qquad \langle f, g \rangle = \sum_{\mathbf{n}} \int_{\mathcal{D}} f(\mathbf{x}, \mathbf{n})g(\mathbf{x}, \mathbf{n})dxdy.$$

Introduce the quasistationary density ϕ_ϵ, for which

$$(4.26) \qquad\qquad \widehat{L}\phi_\epsilon = 0, \quad \phi_\epsilon(\mathbf{x}, \mathbf{n}) = \mathcal{O}(e^{-C/\epsilon}), \quad \mathbf{x} \in \Gamma, \mathbf{n} \in \Sigma.$$

Application of the divergence theorem to the identity (3.29) shows that

$$(4.27) \qquad\qquad \langle \phi_\epsilon, \widehat{L}^*\xi_0 \rangle = \langle \widehat{L}\phi_\epsilon, \xi_0 \rangle - \int_{\Sigma} (V(\mathbf{x}, \mathbf{n}), \widetilde{V}(\mathbf{x}, \mathbf{n})) \cdot \widehat{\mathbf{s}}dl,$$

where

$$(4.28) \qquad V(\mathbf{x}, \mathbf{n}) = \xi_0(\mathbf{x}, \mathbf{n})v(\mathbf{x}, \mathbf{n})\phi_\epsilon(\mathbf{x}, \mathbf{n}), \quad \widetilde{V}(\mathbf{x}, \mathbf{n}) = \xi_0(\mathbf{x}, \mathbf{n})\widetilde{v}(\mathbf{x}, \mathbf{n})\phi_\epsilon(\mathbf{x}, \mathbf{n}).$$

It follows that

$$(4.29) \qquad\qquad \lambda_0 = -\frac{\sum_{\mathbf{n}} \int_{\Sigma}(V(\mathbf{x}, \mathbf{n}), \widetilde{V}(\mathbf{x}, \mathbf{n})) \cdot \widehat{\mathbf{s}}dl}{\langle \xi_0, \phi_\epsilon \rangle}.$$

The basic steps in the evaluation of λ_0 are identical to the one-population model. However, the detailed calculation is more complicated and requires numerically solving zero energy trajectories of an effective Hamiltonian system, which arises from the WKB approximation.

4.2. WKB method and the quasistationary density. Following along similar lines to the one-population model, we approximate the quasistationary density $\phi_\epsilon(\mathbf{x}, \mathbf{n})$ of the CK equation (4.11) using the WKB method. That is, we seek a solution of the form

$$(4.30) \qquad \phi_\epsilon(\mathbf{x}, \mathbf{n}) = \left[R^{(0)}(\mathbf{x}, \mathbf{n}) + \epsilon R^{(1)}(\mathbf{x}, \mathbf{n}) \right] \exp\left(-\frac{\Phi_0(\mathbf{x}) + \epsilon \Phi_1(\mathbf{x})}{\epsilon} \right).$$

Substituting into (4.11) and collecting leading-order terms in ϵ gives

$$(4.31) \qquad \sum_{\mathbf{m}} A(\mathbf{n}, \mathbf{m}; \mathbf{x}) R^{(0)}(\mathbf{x}, \mathbf{m}) = - \left[\mathcal{P}_x(\mathbf{x}) v(\mathbf{x}, \mathbf{n}) + \mathcal{P}_y(\mathbf{x}) \widetilde{v}(\mathbf{x}, \mathbf{n}) \right] R^{(0)}(\mathbf{x}, \mathbf{n}),$$

where

$$(4.32) \qquad \mathcal{P}_x = \frac{\partial \Phi_0}{\partial x}, \quad \mathcal{P}_y = \frac{\partial \Phi_0}{\partial y}.$$

Given the explicit form of the drift terms $v, \widetilde{v}$, the factor $\mathcal{P}_x v + \mathcal{P}_y \widetilde{v}$ for $(x, y) \in \mathcal{D}$ has at least two components of opposite sign. This is a necessary condition for the existence of a nontrivial positive solution for $R^{(0)}$ in the domain $\mathcal{D}$ according to Theorem 3.1 of [61]. We now make the ansatz

$$(4.33) \qquad R^{(0)}(\mathbf{x}, \mathbf{n}) = \frac{\Lambda_x(\mathbf{x})^{n_x}}{n_x!} \cdot \frac{\Lambda_y(\mathbf{x})^{n_y}}{n_y!}.$$

Substituting into (4.31) and using the explicit expressions for A, v, and $\widetilde{v}$, we find that

$$\left[\frac{F(x)}{\Lambda_x} - 1 \right] n_x + \left[\frac{F(y)}{\Lambda_y} - 1 \right] n_y + \Lambda_x + \Lambda_y - F(x) - F(y)$$

$$(4.34) \qquad = -\mathcal{P}_x[-x + w_{EE} n_x - w_{EI} n_y] - \mathcal{P}_y[-y + w_{IE} n_x - w_{II} n_y].$$

The variables $\mathcal{P}_x$ and $\mathcal{P}_y$ can be determined by canceling terms in n_x and n_y. This yields the pair of simultaneous equations

$$(4.35) \qquad \frac{F(x)}{\Lambda_x} - 1 = -[w_{EE} \mathcal{P}_x + w_{IE} \mathcal{P}_y], \quad \frac{F(y)}{\Lambda_y} - 1 = w_{EI} \mathcal{P}_x + w_{II} \mathcal{P}_y.$$

Substituting back into (4.34) gives

$$(4.36) \qquad x \mathcal{P}_x + y \mathcal{P}_y = \Lambda_x + \Lambda_y - F(x) - F(y).$$

Solving for Λ_x, Λ_y in terms of $\mathcal{P}_x$ and $\mathcal{P}_y$, equation (4.36) can be rewritten as

$$(4.37) \quad \mathcal{H}(x, y, \mathcal{P}_x, \mathcal{P}_y) \equiv -x \mathcal{P}_x - y \mathcal{P}_y - F(x) - F(y) + \Lambda_x(x, \mathcal{P}_x, \mathcal{P}_y) + \Lambda_y(y, \mathcal{P}_x, \mathcal{P}_y) = 0,$$

where

$$(4.38) \qquad \Lambda_x = \frac{F(x)}{1 - w_{EE} \mathcal{P}_x - w_{IE} \mathcal{P}_y}, \quad \Lambda_y = \frac{F(y)}{1 + w_{EI} \mathcal{P}_x + w_{II} \mathcal{P}_y}.$$

Mathematically speaking, (4.37) is identical in form to a stationary Hamilton Jacobi equation for a classical particle moving in the domain $\mathcal{D}$, with $\mathcal{H}$ identified as the Hamiltonian. A trajectory of the particle is given by the solution of Hamilton's equations

$$
\frac{dx}{dt} = \frac{\partial \mathcal{H}}{\partial \mathcal{P}_x}, \quad \frac{dy}{dt} = \frac{\partial \mathcal{H}}{\partial \mathcal{P}_y},
$$

(4.39)
$$
\frac{d\mathcal{P}_x}{dt} = -\frac{\partial \mathcal{H}}{\partial x}, \quad \frac{d\mathcal{P}_y}{dt} = -\frac{\partial \mathcal{H}}{\partial y}.
$$

Here t is treated as a parameterization of trajectories rather than as a real-time variable. Given a solution curve $(x(t), y(t))$, known as a ray, the potential Φ_0 can be determined along the ray by solving the equation

(4.40)
$$
\frac{d\Phi_0}{dt} \equiv \frac{\partial \Phi_0}{\partial x} \frac{dx}{dt} + \frac{\partial \Phi_0}{\partial y} \frac{dy}{dt} = \mathcal{P}_x \frac{dx}{dt} + \mathcal{P}_y \frac{dy}{dt}.
$$

Thus, Φ_0 can be identified as the action along a zero energy trajectory. One can then numerically solve for Φ_0 by considering Cauchy data in a neighborhood of the stable fixed point (x_-, y_-) [55]. We find that Hamilton's equations take the explicit form

$$
\frac{dx}{dt} = -x + w_{EE}F(x) - w_{EI}F(y) + \frac{w_{EE}\mathcal{P}_x + w_{IE}\mathcal{P}_y}{[1 - w_{EE}\mathcal{P}_x - w_{IE}\mathcal{P}_y]^2} w_{EE}F(x)
$$

(4.41)
$$
- \frac{w_{EI}\mathcal{P}_x + w_{II}\mathcal{P}_y}{[w_{EI}\mathcal{P}_x + w_{II}\mathcal{P}_y + 1]^2} w_{EI}F(y),
$$

$$
\frac{dy}{dt} = -y + w_{IE}F(x) - w_{II}F(y) + \frac{w_{EE}\mathcal{P}_x + w_{IE}\mathcal{P}_y}{[1 - w_{EE}\mathcal{P}_x - w_{IE}\mathcal{P}_y]^2} w_{IE}F(x)
$$

(4.42)
$$
- \frac{w_{EI}\mathcal{P}_x + w_{II}\mathcal{P}_y}{[w_{EI}\mathcal{P}_x + w_{II}\mathcal{P}_y + 1]^2} w_{II}F(y),
$$

(4.43)
$$
\frac{d\mathcal{P}_x}{dt} = \mathcal{P}_x - \frac{w_{EE}\mathcal{P}_x + w_{IE}\mathcal{P}_y}{1 - w_{EE}\mathcal{P}_x - w_{IE}\mathcal{P}_y} F'(x),
$$

(4.44)
$$
\frac{d\mathcal{P}_y}{dt} = \mathcal{P}_y + \frac{w_{EI}\mathcal{P}_x + w_{II}\mathcal{P}_y}{w_{EE}\mathcal{P}_x + w_{IE}\mathcal{P}_y + 1} F'(y).
$$

Note that we recover the mean-field equations along the manifold $\mathcal{P}_x = \mathcal{P}_y = 0$ with $\Lambda_x = F(x), \Lambda_y = F(y)$.

It remains to specify Cauchy data for the effective Hamiltonian system. At the stable fixed point, the value of each variable is known with $\mathcal{P}_x = \mathcal{P}_y = 0$ and $(x, y) = (x_-, y_-)$. However, data at a single point is not sufficient to generate a family of rays. Therefore, as is well known in the application of WKB methods [54, 48, 72], it is necessary to specify data on a small ellipse surrounding the fixed point. Thus, Taylor expanding Φ_0 around the fixed point yields, to leading order, the quadratic form

(4.45)
$$
\Phi_0(x, y) \approx \frac{1}{2} \mathbf{z}^T \mathbf{Z} \mathbf{z}, \quad \mathbf{z} = \begin{pmatrix} x - x_- \\ y - y_- \end{pmatrix},
$$

where $\mathbf{Z}$ is the Hessian matrix

$$(4.46) \qquad \mathbf{Z} = \begin{pmatrix} \frac{\partial^2 \Phi_0}{\partial x^2} & \frac{\partial^2 \Phi_0}{\partial x \partial y} \\ \frac{\partial^2 \Phi_0}{\partial y \partial x} & \frac{\partial^2 \Phi_0}{\partial y^2} \end{pmatrix},$$

and we have chosen $\Phi_0(x_-, y_-) = 0$. Cauchy data are specified on the θ-parameterized ellipse

$$(4.47) \qquad \frac{1}{2} \mathbf{z}^T(\theta) \mathbf{Z} \mathbf{z}(\theta) = \chi$$

for a suitably chosen parameter χ that is small enough to generate accurate numerical results, but large enough so that the ellipse can generate trajectories that cover the whole domain $\mathcal{D}$. On the elliptical Cauchy curve, the initial values of $\mathcal{P}_x$ and $\mathcal{P}_y$ are

$$(4.48) \qquad \begin{pmatrix} \mathcal{P}_{x,0}(\theta) \\ \mathcal{P}_{y,0}(\theta) \end{pmatrix} = \mathbf{Z} \begin{pmatrix} x_0(\theta) - x_- \\ y_0(\theta) - y_- \end{pmatrix}.$$

It can be shown that the Hessian matrix satisfies the algebraic Riccati equation [48]

$$(4.49) \qquad \mathbf{Z}\mathbf{B}\mathbf{Z} + \mathbf{Z}\mathbf{C} + \mathbf{C}^T\mathbf{Z} = 0,$$

where

$$(4.50) \qquad \mathbf{B} = \begin{pmatrix} \frac{\partial^2 \mathcal{H}}{\partial \mathcal{P}_x^2} & \frac{\partial^2 \mathcal{H}}{\partial \mathcal{P}_x \partial \mathcal{P}_y} \\ \frac{\partial^2 \mathcal{H}}{\partial \mathcal{P}_y \partial \mathcal{P}_x} & \frac{\partial^2 \mathcal{H}}{\partial \mathcal{P}_y^2} \end{pmatrix}, \quad \mathbf{C} = \begin{pmatrix} \frac{\partial^2 \mathcal{H}}{\partial \mathcal{P}_x \partial x} & \frac{\partial^2 \mathcal{H}}{\partial \mathcal{P}_x \partial y} \\ \frac{\partial^2 \mathcal{H}}{\partial \mathcal{P}_y \partial x} & \frac{\partial^2 \mathcal{H}}{\partial \mathcal{P}_y \partial y} \end{pmatrix}$$

are evaluated at $\mathcal{P}_x = \mathcal{P}_y = 0$ and $(x, y) = (x_-, y_-)$. In order to numerically solve the Riccati equation it is convenient to transform it into a linear problem by making the substitution $\mathbf{Q} = \mathbf{Z}^{-1}$:

$$(4.51) \qquad \mathbf{B} + \mathbf{C}\mathbf{Q} + \mathbf{Q}\mathbf{C}^T = 0.$$

Proceeding to the next order in the WKB solution of (4.11), we find

$$\sum_{\mathbf{m}} \left[A(\mathbf{n}, \mathbf{m}; \mathbf{x}) + \delta_{\mathbf{n},\mathbf{m}} (\mathcal{P}_x(\mathbf{x}) v(\mathbf{x}, \mathbf{n}) + \mathcal{P}_y(\mathbf{x}) \widetilde{v}(\mathbf{x}, \mathbf{n})) \right] R^{(1)}(\mathbf{x}, \mathbf{m})$$

$$= \frac{\partial [v(\mathbf{x}, \mathbf{n}) R^{(0)}(\mathbf{x}, \mathbf{n})]}{\partial x} + \frac{\partial [\widetilde{v}(\mathbf{x}, \mathbf{n}) R^{(0)}(\mathbf{x}, \mathbf{n})]}{\partial y}$$

$$(4.52) \qquad - \left(\frac{\partial \Phi_1}{\partial x} v(\mathbf{x}, \mathbf{n}) + \frac{\partial \Phi_1}{\partial y} \widetilde{v}(\mathbf{x}, \mathbf{n}) \right) R^{(0)}(\mathbf{x}, \mathbf{n}).$$

Since the operator $A(\mathbf{n}, \mathbf{m}; \mathbf{x}) + \delta_{\mathbf{n},\mathbf{m}} (\mathcal{P}_x(\mathbf{x}) v(\mathbf{x}, \mathbf{n}) + \mathcal{P}_y(\mathbf{x}) \widetilde{v}(\mathbf{x}, \mathbf{n}))$ has the unique right null vector $R^{(0)}$, its left null space is also one-dimensional spanned by $S(\mathbf{x}, \mathbf{n})$. The Fredholm alternative theorem then yields the solvability condition

$$\sum_{\mathbf{n}} S(\mathbf{x}, \mathbf{n}) \left[\frac{\partial v(\mathbf{x}, \mathbf{n}) R^{(0)}(\mathbf{x}, \mathbf{n})}{\partial x} + \frac{\partial \widetilde{v}(\mathbf{x}, \mathbf{n}) R^{(0)}(\mathbf{x}, \mathbf{n})}{\partial y} \right]$$

$$(4.53) \qquad = \sum_{\mathbf{n}} S(\mathbf{x}, \mathbf{n}) \left[\frac{\partial \Phi_1}{\partial x} v(\mathbf{x}, \mathbf{n}) + \frac{\partial \Phi_1}{\partial y} \widetilde{v}(\mathbf{x}, \mathbf{n}) \right] R^{(0)}(\mathbf{x}, \mathbf{n}),$$

with S satisfying

$$(4.54) \qquad \sum_{\mathbf{n}} S(\mathbf{x}, \mathbf{n}) \left(A(\mathbf{n}, \mathbf{m}; \mathbf{x}) + \delta_{\mathbf{n}, \mathbf{m}} (\mathcal{P}_x(\mathbf{x}) v(\mathbf{x}, \mathbf{n}) + \mathcal{P}_y(\mathbf{x}) \widetilde{v}(\mathbf{x}, \mathbf{n})) \right) = 0.$$

Using the fact that

$$(4.55) \qquad \sum_{\mathbf{n}} S(\mathbf{x}, \mathbf{n}) \left[\frac{dx}{dt} v(\mathbf{x}, \mathbf{n}) - \frac{dy}{dt} \widetilde{v}(\mathbf{x}, \mathbf{n}) \right] R^{(0)}(\mathbf{x}, \mathbf{n}) = 0$$

along trajectories of the Hamiltonian system, we can rewrite the solvability condition as (cf. (3.38))

$$
\begin{aligned}
\frac{d\Phi_1}{dt} &\equiv \frac{\partial \Phi_1}{\partial x} \frac{dx}{dt} + \frac{\partial \Phi_1}{\partial y} \frac{dy}{dt} \\
(4.56) \qquad &= \frac{\dot{x}}{G(\mathbf{x})} \sum_{\mathbf{n}} S(\mathbf{x}, \mathbf{n}) \left[\frac{\partial v(\mathbf{x}, \mathbf{n}) R^{(0)}(\mathbf{x}, \mathbf{n})}{\partial x} + \frac{\partial \widetilde{v}(\mathbf{x}, \mathbf{n}) R^{(0)}(\mathbf{x}, \mathbf{n})}{\partial y} \right],
\end{aligned}
$$

with

$$(4.57) \qquad G(\mathbf{x}) = \sum_{\mathbf{n}} S(\mathbf{x}, \mathbf{n}) v(\mathbf{x}, \mathbf{n}) R^{(0)}(\mathbf{x}, \mathbf{n}).$$

As shown in Appendix A of [55], an equation of this form can be numerically integrated along the trajectories of the underlying Hamiltonian system.

The function $S(\mathbf{x}, \mathbf{n})$ may be solved explicitly by substituting the ansatz

$$(4.58) \qquad S(\mathbf{x}, \mathbf{n}) = \Gamma_x^{n_x}(\mathbf{x}) \cdot \Gamma_y^{n_y}(\mathbf{x})$$

into (4.54) and using the explicit expressions for $A, v, \widetilde{v}$. One finds that

$$
\begin{aligned}
& F(x)[\Gamma_x - 1] + F(y)[\Gamma_y - 1] + n_x \left[\frac{1}{\Gamma_x} - 1 \right] + n_y \left[\frac{1}{\Gamma_y} - 1 \right] \\
(4.59) \qquad &= -\mathcal{P}_x[-x + w_{EE} n_x - w_{EI} n_y] - \mathcal{P}_y[-y + w_{IE} n_x - w_{II} n_y].
\end{aligned}
$$

Canceling the terms in n_x and n_y yields

$$(4.60) \qquad \frac{1}{\Gamma_x} - 1 = -[w_{EE} \mathcal{P}_x + w_{IE} \mathcal{P}_y],$$

$$(4.61) \qquad \frac{1}{\Gamma_y} - 1 = w_{EI} \mathcal{P}_x + w_{II} \mathcal{P}_y.$$

Comparison with (4.35) shows that

$$(4.62) \qquad \Gamma_x = \frac{\Lambda_x}{F(x)}, \quad \Gamma_y = \frac{\Lambda_y}{F(y)},$$

so that

$$(4.63) \qquad \eta_{n_x, n_y} = \left(\frac{\Lambda_x}{F(x)} \right)^{n_x} \cdot \left(\frac{\Lambda_y}{F(y)} \right)^{n_y}.$$

In summary, the quasistationary approximation takes the form

$$(4.64) \qquad \phi_\epsilon(\mathbf{x}, \mathbf{n}) \sim \mathcal{N} \mathrm{e}^{-\Phi_1(\mathbf{x})} \mathrm{e}^{-\Phi_0(\mathbf{x})/\epsilon} R^{(0)}(\mathbf{x}, \mathbf{n}).$$

The normalization factor $\mathcal{N}$ can be approximated using Laplace's method to give

$$(4.65) \qquad \mathcal{N} = \left[\int_{\mathcal{D}} \exp \left[-\frac{\Phi_0(x,y)}{\varepsilon} - \Phi_1(x,y) \right] \right]^{-1} \sim \frac{\sqrt{\det(\mathbf{Z}(x_-, y_-))}}{2\pi\epsilon},$$

where $\mathbf{Z}$ is the Hessian matrix

$$(4.66) \qquad \mathbf{Z} = \begin{pmatrix} \frac{\partial^2 \Phi_0}{\partial x^2} & \frac{\partial^2 \Phi_0}{\partial x \partial y} \\ \frac{\partial^2 \Phi_0}{\partial y \partial x} & \frac{\partial^2 \Phi_0}{\partial y^2} \end{pmatrix},$$

and we have chosen $\Phi_0(x_-, y_-) = 0 = \Phi_1(x_-, y_-)$.

4.3. Perturbation analysis of the adjoint eigenfunction. Since λ_0 is exponentially small, the leading-order equation for the adjoint eigenfunction ξ_0 is

$$(4.67) \qquad \epsilon \left[v(\mathbf{x}, \mathbf{n}) \frac{\partial}{\partial x} + \widetilde{v}(\mathbf{x}, \mathbf{n}) \frac{\partial}{\partial y} \right] \xi_0(\mathbf{x}, \mathbf{n}) + \sum_{\mathbf{m}} A(\mathbf{m}, \mathbf{n}; \mathbf{x}) \xi_0(\mathbf{x}, \mathbf{m}) = 0,$$

supplemented by the absorbing boundary conditions

$$(4.68) \qquad \xi_0(\mathbf{x}, \mathbf{n}) = 0, \quad \mathbf{x} \in \Sigma,$$

for all (n_x, n_y) such that

$$(4.69) \qquad (v(x, n_x, n_y), \widetilde{v}(y, n_x, n_y)) \cdot \widehat{\mathbf{s}} > 0.$$

Following along similar lines to [55], we introduce a new coordinate system $\tau = \tau(x, y), \sigma = \sigma(x, y)$ such that τ parameterizes the separatrix $(x, y) \in \Sigma$ and σ is a local coordinate along the normal $\hat{\mathbf{s}}$ of Σ. We scale σ so that $(\partial x / \partial \sigma, \partial y / \partial \sigma) = \hat{\mathbf{s}}$ at $\sigma = 0$. Equation (4.67) becomes

$$(4.70) \qquad \epsilon \left[v_\tau \frac{\partial}{\partial \tau} + v_\sigma \frac{\partial}{\partial \sigma} \right] \xi_0(\mathbf{x}, \mathbf{n}) + \sum_{\mathbf{m}} A(\mathbf{m}, \mathbf{n}; \mathbf{x}) \xi_0(\mathbf{x}, \mathbf{m}) = 0,$$

where

$$(4.71) \qquad v_\tau = \frac{\partial \tau}{\partial x} v + \frac{\partial \tau}{\partial y} \widetilde{v}, \quad v_\sigma = \frac{\partial \sigma}{\partial x} v + \frac{\partial \sigma}{\partial y} \widetilde{v},$$

and all terms are rewritten as functions of τ, σ. Thus, $f(\sigma, \tau) = f(x(\sigma, \tau), y(\sigma, \tau))$, etc. As a first attempt at obtaining an approximation for ξ_0, we introduce a boundary layer around Γ by setting $\sigma = \epsilon z$ and $Q(z, \tau, \mathbf{n}) = \xi_0(\epsilon z, \tau, \mathbf{n})$. To leading order, (4.70) becomes

$$(4.72) \qquad \left[v_\sigma(0, \tau, \mathbf{n}) \frac{\partial}{\partial z} \right] Q(z, \tau, \mathbf{n}) + \sum_{\mathbf{m}} A(\mathbf{m}, \mathbf{n}; \mathbf{x}) Q(z, \tau, \mathbf{m}) = 0.$$

The inner solution has to be matched with the outer solution $\xi_0(\mathbf{x}, \mathbf{n}) = 1$, which means

$$\lim_{z \to \infty} Q(z, \tau, \mathbf{n}) = 1. \tag{4.73}$$

We now introduce the eigenfunction expansion (cf. (3.48))

$$Q(z, \tau, \mathbf{n}) = c_0(\tau) + \sum_r c_r(\tau) S_r(0, \tau, \mathbf{n}) e^{-\mu_r(0,\tau)z}, \tag{4.74}$$

where the eigenpair (S_r, μ_r) satisfies

$$\mu_r(\sigma, \tau) v_\sigma(\sigma, \tau, \mathbf{n}) S_r(\sigma, \tau, \mathbf{n}) = \sum_{\mathbf{m}} A(\mathbf{m}, \mathbf{n}; \sigma, \tau) S_r(\sigma, \tau, \mathbf{m}). \tag{4.75}$$

We take $S_0 = 1$ and $\mu_0 = 0$. In order that the solution remain bounded as $z \to \infty$ and fixed τ, we require that $c_r(\tau) = 0$ if $\mathrm{Re}[\mu_r(0, \tau)] < 0$. Suppose that the boundary conditions (4.68) for fixed τ generate a system of linear equations for the unknown coefficients $c_r(\tau)$ of codimension k. One of the coefficients is determined by matching the outer solution, which suggests that there are $k - 1$ eigenvalues with negative real part for each τ; the corresponding coefficients c_r are set to zero.

Analogous to the one-population model, an additional eigenvalue μ_1, say, vanishes at the saddle point $(0, \tau_*)$ on the separatrix. In order to show this, suppose that

$$\mu_1 = -\frac{\partial \Phi_0}{\partial \sigma}. \tag{4.76}$$

Substitution into (4.75) for $r = 1$ and fixed τ then yields an equation identical in form to (4.54), and we can identify $S_1 = S$. Since $\mathcal{P}_x$ and $\mathcal{P}_y$ vanish at $(0, \tau_*)$, it follows that $\mu_1(0, \tau_*) = 0$. Hence, the solution at τ_* has to include a secular term involving the generalized eigenvector $\widehat{S}$, where

$$\sum_{\mathbf{m}} A(\mathbf{m}, \mathbf{n}; 0, \tau_*) \widehat{S}(0, \tau_*, \mathbf{m}) = -v_\sigma(0, \tau_*, \mathbf{n}). \tag{4.77}$$

The Fredholm alternative theorem ensures that a solution exists. Setting $\widehat{S}(0, \tau^*; \mathbf{n}) = \zeta(\mathbf{n})$, we have

$$\begin{aligned}
&F(x)\zeta(n_x + 1, n_y) + F(y)\zeta(n_x, n_y + 1) + n_x\zeta(n_x - 1, n_y) + n_y\zeta(n_x, n_y - 1) \\
&\quad -[F(x) + F(y) + n_x + n_y]\zeta(n_x, n_y) \\
&= s_x[x - w_{EE}n_x + w_{EI}n_y] + s_y[y - w_{IE}n_x + w_{II}n_y].
\end{aligned} \tag{4.78}$$

This has a solution of the form $\zeta(n_x, n_y) = \mathcal{A}_x n_x + \mathcal{A}_y n_y$, with the coefficients $\mathcal{A}_x, \mathcal{A}_y$ determined by canceling linear terms in n_x, n_y. Thus

$$\zeta(n_x, n_y) = [w_{EE}s_x + w_{IE}s_y]n_x - [w_{EI}s_x + w_{II}s_y]n_y. \tag{4.79}$$

Given $\widehat{S}$, (4.74) becomes

$$Q(z, \tau_*, \mathbf{n}) = c_0(\tau_*) + c_1(\tau_*)(\widehat{S}(z, \tau^*, \mathbf{n}) - z) + \sum_{r \geq 2} c_r(\tau_*) S_r(0, \tau_*, \mathbf{n}) e^{-\mu_r(0,\tau_*)z}. \tag{4.80}$$

The presence of the secular term implies that the solution is unbounded so it has to be eliminated using a modified stretch variable $\sigma = \sqrt{\epsilon}z$ [56, 55]. Proceeding along similar lines to the one-population case, we find that

$$(4.81) \qquad c_1(\tau_*) \sim \sqrt{\frac{2\epsilon|\partial_\sigma \mu_1(0, \tau_*)|}{\pi}}.$$

4.4. Principal eigenvalue. We now return to the expression for the principal eigenvalue λ_0 given by (4.29). Simplifying the denominator by using the outer solution $\boldsymbol{\xi}_0 \sim \mathbf{1}$ and using the WKB approximation of $\boldsymbol{\phi}_\epsilon$, (4.64), gives

$$(4.82) \qquad \lambda_0 = -\mathcal{N} \int_\Gamma \mathrm{e}^{-\Phi_1(\mathbf{x})} \mathrm{e}^{-\Phi_0(\mathbf{x})/\epsilon} \left(U(\mathbf{x}), \widetilde{U}(\mathbf{x}) \right) \cdot \widehat{\mathbf{s}} dl,$$

with

$$(4.83) \qquad U(\mathbf{x}) = \sum_{\mathbf{n}} \widehat{S}(\mathbf{x}, \mathbf{n}) v(\mathbf{x}, \mathbf{n}) R^{(0)}(\mathbf{x}, \mathbf{n}), \quad \widetilde{U}(\mathbf{x}) = \sum_{\mathbf{n}} \widehat{S}(\mathbf{x}, \mathbf{n}) \widetilde{v}(\mathbf{x}, \mathbf{n}) R^{(0)}(\mathbf{x}, \mathbf{n}).$$

Changing to the (σ, τ) coordinate system and evaluating the line integral by applying Laplace's method around the saddle point $(0, \tau^*)$ then gives

$$\lambda_0 \sim \mathcal{N} B(\tau_*) c_1(\tau_*) \mathrm{e}^{-\Phi_1(0, \tau_*)} \mathrm{e}^{-\Phi_0(0, \tau_*)/\epsilon} \int_\Gamma \exp\left(-\frac{1}{2\epsilon} \partial_{\tau\tau} \Phi_0(0, \tau_*) (\tau - \tau_*)^2 \right) d\tau,$$

$$\sim B(\tau_*) c_1(\tau_*) \mathrm{e}^{-\Phi_1(0, \tau_*)} \mathrm{e}^{-\Phi_0(0, \tau_*)/\epsilon} \sqrt{\frac{2\pi}{\partial_{\tau\tau} \Phi_0(0, \tau_*)}} \frac{\sqrt{\det(\mathbf{Z}(x_-, y_-))}}{2\pi\epsilon}$$

$$(4.84) \qquad \sim \frac{1}{\pi} B(\tau_*) \mathrm{e}^{-\Phi_1(0, \tau_*)} \mathrm{e}^{-\Phi_0(0, \tau_*)/\epsilon} \sqrt{\frac{\partial_{\sigma\sigma} \Phi_0(0, \tau_*) \det(\mathbf{Z}(x_-, y_-))}{\partial_{\tau\tau} \Phi_0(0, \tau_*)}},$$

where we have used (4.65), (4.80), (4.81), and

$$(4.85) \qquad B(\tau_*) = -\left(U(0, \tau_*), \widetilde{U}(0, \tau_*) \right) \cdot \widehat{\mathbf{s}}.$$

4.5. Numerical results. The rays $(x(t), y(t))$ (i.e., solutions to Hamilton's equations (4.39) in the (x, y)-plane) have an important physical meaning. The trajectory of the ray is the most likely trajectory or path leading away from a point in the neighborhood of a stable fixed point [24]. The rays $(x(t), y(t))$ shown in Figure 6 are obtained by integrating the characteristic equations (4.41)–(4.44). These trajectories are valid only in one direction: away from the stable fixed points. For the parameter values considered in Figure 6, rays originating from each stable fixed point cover separate regions, so that the most likely paths between points in each region are connected by deterministic trajectories starting at the boundary between the two regions. Note that this boundary is not the separatrix (gray curve). If a trajectory crosses the separatrix away from the saddle, it is most likely to cross the separatrix above the saddle when starting from the left fixed point and below the saddle when starting from the right fixed point (see Figure 7). At first glance, this suggests that if the trajectory starts at the
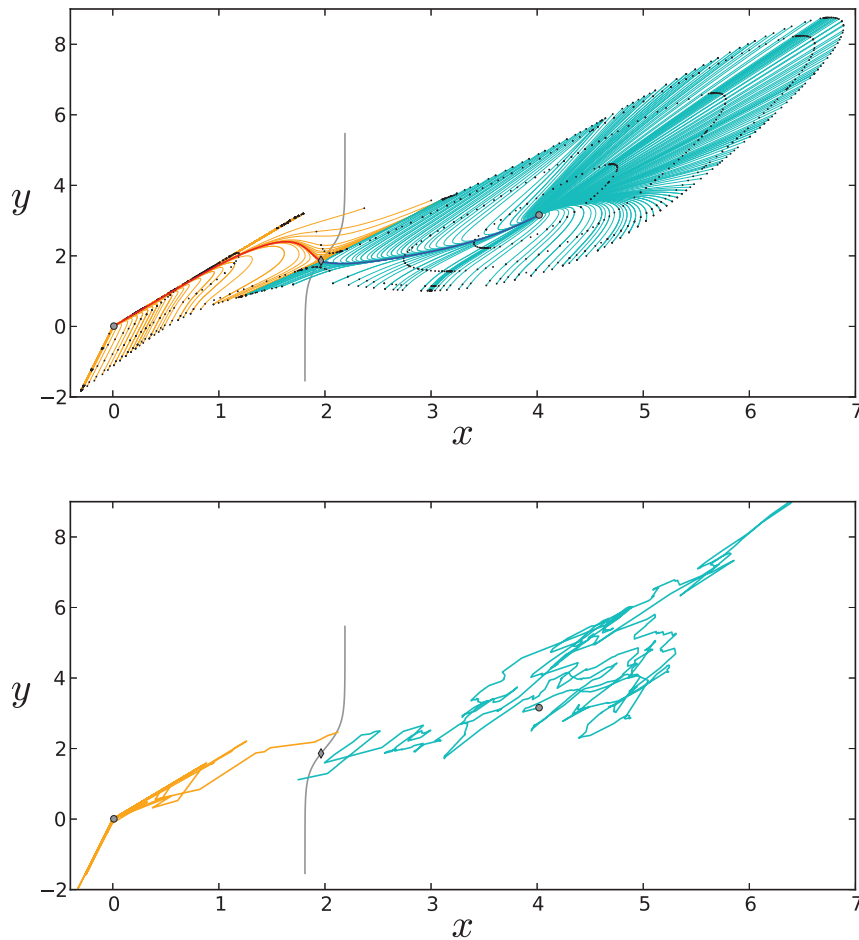
Figure 6. (a) *Characteristic paths of maximum likelihood for the two-dimensional model. Rays originating from the left (right) stable fixed point are shown in orange (cyan), with the ray connecting to the saddle shown in red (blue). The gray curve is the separatrix Σ. Level curves of constant $\Phi(x, y)$ are shown as black dots. Each ray has four dots for different values of $\Phi(x, y)$. Rays originating from the left fixed point have dots at $\Phi = 0.1, 0.2, \Phi_* + 0.01, \Phi_* + 0.02$, and rays originating from the right fixed point have dots at $\Phi = 0.19, 0.23, 0.28, 0.30$, where $\Phi_* = \Phi(x_*, y_*) = 0.28$. All rays terminate at $\Phi = \Phi_* + 0.02$. (b) Sample trajectories of the two-population velocity jump Markov process, whose associated probability density evolves according to (4.1), are computed using the Gillespie algorithm with $\epsilon = 0.05$ and $N\Delta t = 1$. (The maximum likelihood paths are independent of ϵ.) Other parameter values are the same as in Figure 5. Details of the simulations are given in section 4.6.*

left fixed point, say, it is more likely to cross above the saddle, continue along a deterministic trajectory to the right fixed point, and then cross the separatrix below the saddle than it is to directly cross below the saddle. This is counterintuitive because it would seem more likely for a single rare, metastable crossing event to lead to a point near the separatrix than two rare events occurring in sequence. However, as shown in [48], rays can also originate from the saddle point, which cross the separatrix in the direction opposite those originating at the stable fixed points.
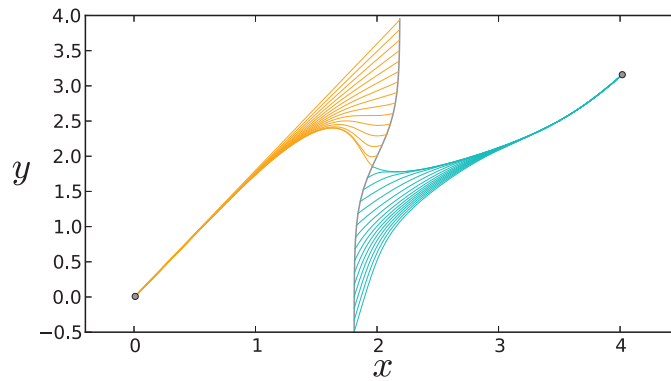
Figure 7. *Maximum likelihood trajectories crossing the separatrix.*
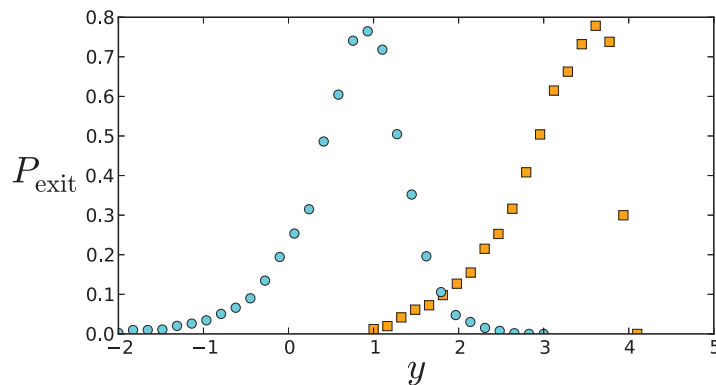
Figure 8. *The probability density for the exit point (y coordinate) where the separatrix is crossed by an exiting trajectory. Results are obtained by 10^2 Monte Carlo simulation with the same parameters as used in Figure 5, with $\epsilon = 0.08$. Orange squares show trajectories from the left well, and cyan circles show trajectories from the right well.*

In Figure 8, the probability density function for the y coordinate of the point on the separatrix reached by an exit trajectory is shown for each well (squares show the histogram for exit from the left well and, likewise, circles for the right well). Each density function is peaked away from the saddle point, showing a phenomenon known as saddle-point avoidance [48, 72]. As $\epsilon \to 0$, the two peaks merge at the saddle point. Although we expect the saddle point to be the most likely exit point since it is the point on the separatrix where the potential Φ takes its minimum value, our results show that this is not necessarily true. Even though the most likely exit point is shifted from the saddle, the value of potential at the saddle point still dominates the mean first exit time. In Figure 9, the mean exit time from each of the two-dimensional potential wells (see Figure 6) is shown. Solid lines show the analytical approximation $T \sim 1/\lambda_0$, where λ_0 is given by (4.84), and circles show averaged Monte Carlo simulations. As in Figure 3, the slope T on a log scale as a function of $1/\epsilon$ is determined by Φ evaluated at the saddle point.
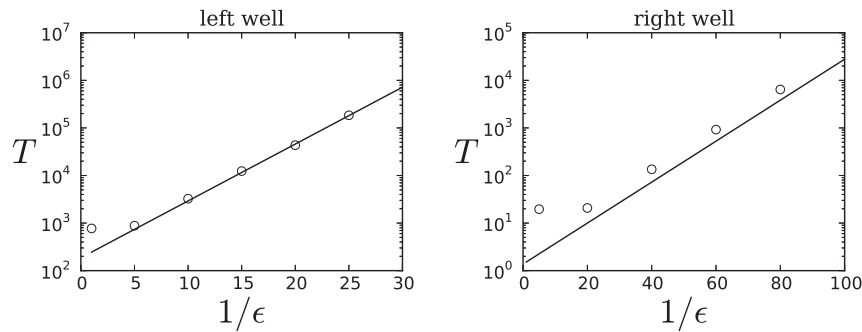
Figure 9. *Mean exit time from the left and right wells. Parameter values are the same as in Figure 5. Solid lines show the analytical approximation $T \sim 1/\lambda_0$, where λ_0 is given by (4.84), and circles show 80 averaged Monte Carlo simulations.*

4.6. Notes on Monte Carlo simulations. Monte Carlo simulations were carried out using the Gillespie algorithm. The Gillespie algorithm evolves the process by computing random jump times and state transitions. The piecewise deterministic Markov process considered here involves three basic steps. First, the next jump time, τ, is generated using the waiting time distribution,

$$(4.86) \qquad \psi_n(t) = \exp\left[-\int_0^t W_n(t')dt'\right],$$

where $W_n(t) = F(u(t)) + n$. Second, the deterministic variable u is integrated forward in time until the next jump time is reached:

$$(4.87) \qquad u(\tau) = u(0) + \int_0^\tau (wn - u(t))dt = (u(0) - wn)e^{-\tau} + wn.$$

Third, the state that the system jumps to at the next jump time is generated. In practice, steps one and two must be performed simultaneously if the rate for the next jump time depends on u. Since the transition rates are functions of u, the standard Gillespie algorithm, which uses exponential random variables, does not apply. The transitions rates are functions of time since u is time dependent between jumps in the internal state. To see this suppose the transition rate W_n is independent of time. Then the exponential random variable τ is given by

$$(4.88) \qquad \tau = -\log(Y)/W_n,$$

where Y is a computer-generated, uniform random variable. On the other hand, if the transition rate depends on u, we have that τ is given implicitly by

$$(4.89) \qquad \int_0^\tau W_n(t|u(0))dt = -\log(Y).$$

Notice that the rate depends on the value of u at the beginning of the jump interval, which we denote as $u(0)$. That is, if we denote the sequence of jump times as $\{\tau_j\}_{j \geq 0}$, then when generating τ_j via (4.89), we set $u(0) = u(\tau_{j-1})$.

Solving (4.89) for τ is much easier if the integral can be evaluated explicitly; the solution requires a simple Newton root-finding algorithm [61]. However, in this case we cannot explicitly evaluate the integral. Instead, we use a quadrature method (we use trapezoidal rule, but it is very simple to implement a higher order method) to integrate the left-hand side of (4.89) forward in time with time step δt. Let

$$(4.90) \qquad \mathcal{W}_k = \frac{\delta t}{2} \sum_{l=0}^{k} (W_n(l\delta t) + W_n((l+1)\delta t)).$$

Then the integration proceeds until

$$(4.91) \qquad \mathcal{W}_{\hat{k}-1} + \log(Y) < 0, \quad \mathcal{W}_{\hat{k}} + \log(Y) > 0.$$

A rough estimate of the jump time is $\tau \approx \hat{k}\delta t$. In practice, once the time step $\hat{k}$ is reached and (4.91) is true, we reverse the integration to $\mathcal{W}_{\hat{k}-1}$ and refine the time step $\delta t \to \delta t/2$. We repeat this process until $\delta t <$ thresh.

5. Discussion. In this paper we developed a generalization of the neural master equation [17, 7, 18], based on a velocity jump Markov process that couples synaptic and spiking dynamics at the population level. There were two distinct time-scales in the model, corresponding to the relaxation times τ and τ_a of the synaptic and spiking dynamics, respectively. In the limit $\tau \to 0$, we recovered the neural master equation operating in a Poisson-like regime, whereas in the limit $\tau_a \to 0$ we obtained deterministic mean-field equations for the synaptic currents. Hence, one additional feature of our model is that it provides a prescription for constructing a stochastic population model that reduces to a current-based model, rather than an activity-based model, in the mean-field limit.

We focused on the particular problem of escape from a metastable state, for which standard diffusion-like approximations break down. We showed how WKB methods and singular perturbation theory could be adapted to solve the escape problem for a velocity jump Markov process, extending recent studies of stochastic ion channels. For concreteness, we assumed that the network operated in the regime $\tau_a/\tau = \epsilon \ll 1$, which meant that transitions between different discrete states of population spiking activity were relatively fast. In this regime, the thermodynamic limit $N \to \infty$ was not a mean-field limit, rather it simplified the analysis since the quasi-steady-state density was Poisson. It would be interesting to consider other parameter regimes in subsequent work. First, we could model the discrete Markov process describing the spiking dynamics using the Bressloff version of the master equation [7]. There would then be two small parameters in the model, namely, ϵ and $1/N$, so one would need to investigate the interplay between the system size expansion for large but finite N and the quasi-steady-state approximation for small ϵ. Another possible scenario (though less plausible physiologically speaking) would be fast synaptic dynamics with $\tau \ll \tau_a$. In this case, mean-field equations are obtained in the thermodynamic limit. Finally, it would be interesting to extend our methods to analyze the effects of noise when the underlying deterministic system exhibits more complicated dynamics such as limit cycle oscillations. As we commented in the main text, the two-population model of excitatory and inhibitory neurons is a canonical circuit for generating population-level oscillations.

Finally, it is important to emphasize that the neural master equation and its generalizations are phenomenological models of stochastic neuronal population dynamics. Although one can give a heuristic derivation of these models [9], there is currently no systematic procedure for deriving them from physiologically based microscopic models, except in a few special cases. Nevertheless, stochastic hybrid models are emerging in various applications within neuroscience, so that the analytical techniques presented in this paper are likely to be of increasing importance.

REFERENCES

[1] L. F. ABBOTT AND C. VAN VRESSWIJK, *Asynchronous states in networks of pulse-coupled oscillators*, Phys. Rev. E, 48 (1993), pp. 1483–1490.

[2] J. BALADRON, D. FASOLI, O. FAUGERAS, AND J. TOUBOUL, *Mean field description of and propagation of chaos in recurrent multipopulation networks of Hodgkin-Huxley and FitzHugh-Nagumo neurons*, J. Math. Neuro., 2 (2012), 10.

[3] R. BLAKE AND H. R. WILSON, *Binocular vision*, Vis. Research, 51 (2011), pp. 754–770.

[4] R. P. BOLAND, T. GALLA, AND A. J. MCKANE, *How limit cycles and quasi-cycles are related in systems with intrinsic noise*, J. Stat. Mech., 2008 (2008), P09001.

[5] R. BORISYUK AND A. B. KIRILLOV, *Bifurcation analysis of a neural network model*, Biol. Cybern., 66 (1992), pp. 319–325.

[6] S. E. BOUSTANI AND A. DESTEXHE, *A master equation formalism for macroscopic modeling of asynchronous irregular activity states*, Neural Comput., 21 (2009), pp. 46–100.

[7] P. C. BRESSLOFF, *Stochastic neural field theory and the system-size expansion*, SIAM J. Appl. Math., 70 (2009), pp. 1488–1521.

[8] P. C. BRESSLOFF, *Metastable states and quasicycles in a stochastic Wilson-Cowan model of neuronal population dynamics*, Phys. Rev. E, 85 (2010), 051903.

[9] P. C. BRESSLOFF, *Spatiotemporal dynamics of continuum neural fields*, J. Phys. A, 45 (2012), 033001.

[10] P. C. BRESSLOFF AND S. COOMBES, *Dynamics of strongly coupled spiking neurons*, Neural Comput., 12 (2000), pp. 91–129.

[11] P. C. BRESSLOFF AND J. M. NEWBY, *Quasi-steady state analysis of motor-driven transport on a two-dimensional microtubular network*, Phys. Rev. E, 83 (2011), 061139.

[12] P. C. BRESSLOFF AND M. WEBBER, *Neural field model of binocular rivalry waves*, J. Comput. Neurosci., 32 (2012), pp. 233–252.

[13] N. BRUNEL, *Dynamics of sparsely connected networks of excitatory and inhibitory spiking neurons*, J. Comput. Neurosci., 8 (2000), pp. 183–208.

[14] N. BRUNEL AND V. HAKIM, *Fast global oscillations in networks of integrate-and-fire neurons with low firing rates*, Neural Comput., 11 (1999), pp. 1621–1671.

[15] E. BUCKWAR AND M. G. RIEDLER, *An exact stochastic hybrid model of excitable membranes including spatio-temporal evolution*, J. Math. Biol., 63 (2011), pp. 1051–1093

[16] E. BUCKWAR AND M. G. RIEDLER, *Laws of large numbers and Langevin approximations for stochastic neural field equations*, J. Math. Neurosci., 3 (2012), 1.

[17] M. BUICE AND J. D. COWAN, *Field-theoretic approach to fluctuation effects in neural networks*, Phys. Rev. E, 75 (2007), 051919.

[18] M. BUICE, J. D. COWAN, AND C. C. CHOW, *Systematic fluctuation expansion for neural network activity equations*, Neural Comp., 22 (2010), pp. 377–426.

[19] M. A. BUICE AND C. C. CHOW, *Effective stochastic behavior in dynamical systems with incomplete information*, Phys. Rev. E, 84 (2011), 051120.

[20] D. CAI, L. TAO, M. SHELLEY, AND D. W. MCLAUGHLIN, *An effective kinetic representation of fluctuation-driven neuronal networks with application to simple and complex cells in visual cortex*, Proc. Natl. Acad. Sci. USA, 101 (2004), pp. 7757–7562.

[21] A. COMPTE, M. V. SANCHEZ-VIVES, D. A. MCCORMICK, AND X.-J. WANG, *Cellular and network mechanisms of slow oscillatory activity (< 1 Hz) and wave propagations in a cortical network model*,

J. Neurophysiol., 89 (2003), pp. 2707–2725.

[22] G. Deco, V. K. Jirsa, and A. R. McIntosh, *Emerging concepts for the dynamical organization of resting-state activity in the brain*, Nat. Rev. Neurosci., 12 (2011), pp. 43–56.

[23] A. Destexhe and D. Contreras, *Neuronal computations with stochastic network states*, Science, 314 (2006), pp. 85–90.

[24] M. I. Dykman, E. Mori, J. Ross, and P. M. Hunt, *Large fluctuations and optimal paths in chemical kinetics*, J. Chem. Phys. A, 100 (1994), pp. 5735–5750.

[25] G. B. Ermentrout, *Reduction of conductance-based models with slow synapses to neural nets*, Neural Comput., 6 (1994), pp. 679–695.

[26] G. B. Ermentrout, *Neural networks as spatio-temporal pattern-forming systems*, Rep. Prog. Phys., 61 (1998), pp. 353–430.

[27] G. B. Ermentrout and D. Terman, *Mathematical Foundations of Neuroscience*, Springer, Berlin, 2010.

[28] A. A. Faisal, L. P. J. Selen, and D. M. Wolpert, *Noise in the nervous system*, Nat. Rev. Neurosci., 9 (2008), p. 292.

[29] O. Faugeras, J. Touboul, and B. Cessac, *A constructive mean-field analysis of multi-population neural networks with random synaptic weights and stochastic inputs*, Frontiers Comput. Neurosci., 3 (2009), pp. 1–28.

[30] J. Feng and T. G. Kurtz, *Large Deviations for Stochastic Processes*, Math. Surveys Monogr. 131, AMS, Providence, RI, 2006.

[31] M. I. Freidlin and A. D. Wentzell, *Random Perturbations of Dynamical Systems*, 2nd ed., Springer, New York, 1998.

[32] A. Friedman and G. Craciun, *A model of intracellular transport of particles in an axon*, J. Math. Biol., 51 (2005), pp. 217–246.

[33] A. Friedman and B. Hu, *Uniform convergence for approximate traveling waves in linear reaction-hyperbolic systems*, Indiana Univ. Math. J., 56 (2007), pp. 2133–2158.

[34] C. W. Gardiner, *Handbook of Stochastic Methods*, 4th ed., Springer, Berlin, 2009.

[35] W. Gerstner and W. Kistler, *Spiking Neuron Models*, Cambridge University Press, Cambridge, UK, 2002.

[36] W. Gerstner and J. L. Van Hemmen, *Coherence and incoherence in a globally coupled ensemble of pulse-emitting units*, Phys. Rev. Lett., 71 (1993), pp. 312–315.

[37] E. R. Grannan, D. Kleinfeld, and H. Sompolinsky, *Stimulus-dependent synchronization of neuronal assemblies*, Neural Comput., 5 (1993), pp. 550–569.

[38] B. Gutkin, C. R. Laing, C. L. Colby, C. C. Chow, and G. B. Ermentrout, *Turning on and off with excitation: The role of spike-timing asynchrony and synchrony in sustained neural activity*, J. Comput. Neurosci., 11 (2001), pp. 121–134.

[39] P. Haangi, H. Grabert, P. Talkner, and H. Thomas, *Bistable systems: Master equation versus Fokker–Planck modeling*, Z. Physik B, 28 (1984), p. 135.

[40] T. Hillen and H. G. Othmer, *The diffusion limit of transport equations derived from velocity-jump processes*, SIAM J. Appl. Math., 61 (2000), pp. 751–775.

[41] J. P. Keener and J. M. Newby, *Perturbation analysis of spontaneous action potential initiation by stochastic ion channels*, Phys. Rev. E, 84 (2011), 011918.

[42] T. G. Kurtz, *Limit theorems for a sequence of jump Markov processes approximating ordinary differential equations*, J. Appl. Probab., 8 (1971), pp. 344–356.

[43] T. G. Kurtz, *Limit theorems and diffusion approximations for density dependent Markov chains*, Math. Programming Stud., 5 (1976), pp. 67–78.

[44] C. R. Laing and C. C. Chow, *A spiking neuron model for binocular rivalry*, J. Comput. Neurosci., 12 (2002), pp. 39–53.

[45] C. R. Laing and G. J. Lord, *Stochastic Methods in Neuroscience*, Oxford University Press, Oxford, 2009.

[46] D. Ludwig, *Persistence of dynamical systems under random perturbations*, SIAM Rev., 17 (1975), pp. 605–640.

[47] C. Ly and D. Tranchina, *Critical analysis of a dimension reduction by a moment closure method in a population density approach to neural network modeling*, Neural Comput., 19 (2007), pp. 2032–2092.

[48] R. S. MAIER AND D. L. STEIN, *Limiting exit location distributions in the stochastic exit problem*, SIAM J. Appl. Math., 57 (1997), pp. 752–790.

[49] B. J. MATKOWSKY AND Z. SCHUSS, *The exit problem for randomly perturbed dynamical systems*, SIAM J. Appl. Math., 33 (1977), pp. 365–382.

[50] M. MATTIA AND P. D. GUIDICE, *Population dynamics of interacting spiking neurons*, Phys. Rev. E, 66 (2002), 051917.

[51] A. J. McKANE, J. D. NAGY, T. J. NEWMAN, AND M. O. STEFANINI, *Amplified biochemical oscillations in cellular systems*, J. Stat. Phys., 128 (2007), pp. 165–191.

[52] C. MEYER AND C. VAN VREESWIJK, *Temporal correlations in stochastic networks of spiking neurons*, Neural Comput., 14 (2002), pp. 369–404.

[53] R. MORENO-BOTE, J. RINZEL, AND N. RUBIN, *Noise-induced alternations in an attractor network model of perceptual bistability*, J. Neurophysiol., 98 (2007), pp. 1125–1139.

[54] T. NAEH, M. M. KŁOSEK, B. J. MATKOWSKY, AND Z. SCHUSS, *A direct approach to the exit problem*, SIAM J. Appl. Math., 50 (1990), pp. 595–627.

[55] J. NEWBY AND J. CHAPMAN, *Metastable Behavior in Markov Processes with Internal States*, preprint, arXiv:1304.6957, 2013.

[56] J. M. NEWBY, *Isolating intrinsic noise sources in a stochastic genetic switch*, Phys. Biol., 9 (2012), 026002.

[57] J. M. NEWBY AND P. C. BRESSLOFF, *Directed intermittent search for a hidden target on a dendritic tree*, Phys. Rev. E, 80 (2009), 021913.

[58] J. M. NEWBY AND P. C. BRESSLOFF, *Local synaptic signalling enhances the stochastic transport of motor-driven cargo in neurons*, Phys. Biol., 7 (2010), 036004.

[59] J. M. NEWBY AND P. C. BRESSLOFF, *Quasi-steady state reduction of molecular-based models of directed intermittent search*, Bull. Math. Biol., 72 (2010), pp. 1840–1866.

[60] J. M. NEWBY, P. C. BRESSLOFF, AND J. P. KEENER, *Spontaneous Action Potential Initiation by Fast and Slow Stochastic Ion Channels*, preprint, arXiv:1304.6952, 2013.

[61] J. M. NEWBY AND J. P. KEENER, *An asymptotic analysis of the spatially inhomogeneous velocity-jump process*, Multiscale Model. Simul., 9 (2011), pp. 735–765.

[62] D. NYKAMP AND D. TRANCHINA, *A population density method that facilitates large-scale modeling of neural networks: Analysis and application to orientation tuning*, J. Comput. Neurosci., 8 (2000), pp. 19–50.

[63] T. OHIRA AND J. D. COWAN, *Stochastic neurodynamics and the system size expansion*, in Proceedings of the First International Conference on Mathematics of Neural Networks, S. Ellacott and I. J. Anderson, eds., Academic Press, 1997, pp. 290–294.

[64] A. OMURTAG, B. W. KNIGHT, AND L. SIROVICH, *On the simulation of large populations of neurons*, J. Comput. Neurosci., 8 (2000), pp. 51–63.

[65] H. OTHMER, S. DUNBAR, AND W. ALT, *Models of dispersal in biological systems*, J. Math. Biol., 26 (1988), pp. 263–298.

[66] K. PAKDAMAN, M. THIEULLEN, AND G. WAINRIB, *Fluid limit theorems for stochastic hybrid systems with application to neuron models*, Adv. in Appl. Probab., 42 (2010), pp. 761–794.

[67] G. C. PAPANICOLAOU, *Asymptotic analysis of transport Processes*, Bull. Amer. Math. Soc., 81 (1975), pp. 330–392.

[68] N. PARGA AND L. F. ABBOTT, *Network model of spontaneous activity exhibiting synchronous transitions between up and down states*, Frontiers in Neurosci., 1 (2007), pp. 57–66.

[69] A. V. RANGAN, G. KOVACIC, AND D. CAI, *Kinetic theory for neuronal networks with fast and slow excitatory conductances driven by the same spike train*, Phys. Rev. E, 77 (2008), 041915.

[70] M. C. REED, S. VENAKIDES, AND J. J. BLUM, *Approximate traveling waves in linear reaction-hyperbolic equations*, SIAM J. Appl. Math., 50 (1990), pp. 167–180.

[71] A. RENART, J. DE LA ROCHA, P. BARTHO, L. HOLLENDER, N. PARGA, A. REYES, AND K. D. HARRIS, *The asynchronous state in cortical circuits*, Science, 327 (2010), pp. 587–590.

[72] Z. SCHUSS, *Theory and Applications of Stochastic Processes: An Analytical Approach*, Appl. Math. Sci. 120, Springer, New York, 2010.

[73] H. G. SCHUSTER AND P. WAGNER, *A model for neuronal oscillations in the visual cortex. 1. Mean-field theory and derivation of the phase equations*, Biol. Cybern., 64 (1990), pp. 77–82.

[74] A. SHPIRO, R. CURTU, J. RINZEL, AND N. RUBIN, *Balance between noise and adaptation in competition models of perceptual bistability*, J. Comput. Neurosci., 27 (2009), pp. 462–473.

[75] W. R. SOFTKY AND C. KOCH, *Cortical cell should spike regularly but do not*, Neural Comput., 4 (1992), pp. 643–646.

[76] H. SOULA AND C. C. CHOW, *Stochastic dynamics of a finite-size spiking neural network*, Neural Comput., 19 (2007), pp. 3262–3292.

[77] P. S. SWAIN AND A. LONGTIN, *Noise in genetic and neural networks*, Chaos, 16 (2006), 026101.

[78] J. TOUBOUL, G. HERMANN, AND O. FAUGERAS, *Noise-Induced Behaviors in Neural Mean Field Dynamics*, preprint, 2011.

[79] J. D. TOUBOUL AND G. B. ERMENTROUT, *Finite-size and correlation-induced effects in mean-field dynamics*, J. Comput. Neurosci., 31 (2011), pp. 453–484.

[80] H. TOUCHETTE, *The large deviation approach to statistical mechanics*, Phys. Rep., 478 (2009), pp. 1–69.

[81] N. G. VAN KAMPEN, *Stochastic Processes in Physics and Chemistry*, North-Holland, Amsterdam, 1992.

[82] X. J. WANG, *Decision making in recurrent neuronal networks*, Neuron, 60 (2008), pp. 215–234.

[83] M. J. WARD AND J. LEE, *On the asymptotic and numerical-analyses of exponentially ill-conditioned singularly perturbed boundary value problems*, Stud. Appl. Math., 94 (1995), pp. 271–326.

[84] M. WEBBER AND P. C. BRESSLOFF, *The effects of noise on binocular rivalry waves: A stochastic neural field model*, J. Stat. Mech., 2013 (2013), P03001.

[85] S. ZEISLER, U. FRANZ, O. WITTICH, AND V. LIEBSCHER, *Simulation of genetic networks modelled by piecewise deterministic Markov processes*, IET Syst. Bio., 2 (2008), pp. 113–135.